The effect of parameters on the performance of a Fluidized bed reactor and Gasifier

A Project submitted to the
National Institute of Technology, Rourkela
In partial fulfillment of the requirements

Of

Master of Technology (Chemical Engineering)

By

Ms. Brahmotri Sahoo

Roll No. 209CH1060

DEPARTMENT OF CHEMICAL ENGINEERING

NATIONAL INSTITUTE OF TECHNOLOGY, ROURKELA

MAY- 2011

The effect of parameters on the performance of a Fluidized bed reactor and Gasifier

A Project submitted to the
National Institute of Technology, Rourkela
In partial fulfillment of the requirements

Of

Master of Technology (Chemical Engineering)

By

Ms. Brahmotri Sahoo

Roll No. 209CH1060

UNDER THE GUIDANCE OF:

PROF. ABANTI SAHOO

DEPARTMENT OF CHEMICAL ENGINEERING

NATIONAL INSTITUTE OF TECHNOLOGY, ROURKELA

MAY- 2011

National Institute of Technology, Rourkela

CERTIFICATE

This is to certify that the project report on "T**he Effect of Parameters on the performance of a Fluidized Bed Reactor and Gasifier**" submitted by **Ms. Brahmotri Sahoo** to National Institute of Technology, Rourkela under my supervision and is worthy for the partial fulfillment of the degree of Master of Technology (Chemical Engineering) of the Institute. She has fulfilled all the prescribed requirements and the thesis, which is based on candidate's own work, has not been submitted elsewhere.

Supervisor

Prof. Abanti Sahoo

Department of Chemical Engg.

NIT, Rourkela,

769008

National Institute of Technology, Rourkela

ACKNOWLEDGEMENT

I feel immense pleasure and privilege to express my deep sense of gratitude and feel indebted towards all those people who have helped, inspired and encouraged me during the preparation of this thesis.

I would like to thank **Prof. Abanti Sahoo**, who provided me this opportunity to highlight the key aspects of an upcoming technology and guided me during the project work preparation and also to my parents and family members whose love and unconditional support, both on academic and personal front, enabled me to see the light of this day.

Thanking you,

Brahmotri sahoo

Roll No. 209CH1060

CONTENTS

Chapter No.			Title	Page No.
1.			INTRODUCTION	(1-5)
	1.1.		Important Factors to study for the reaction kinetics of a process	2
	1.2.		Process Modeling	3
	1.3.		Applications of Fluidized bed reactor	3
	1.4.		Advantages of Fluidized bed reactor	3-4
	1.5.		Objective of the work	5
2.			LITERATURE SURVEYS	(6-20)
	2.1.		Principles of Fluidized bed reactor	7
	2.2.		Previous work	8-20
3.			EXPERIMENTATION	(21-26)
	3.1.		Types of raw materials used	22
	3.2.		Experimental procedure	22-26
		3.2.1.	Cold Model experimentation	22-24
		3.2.2.	Hot model experimentation	24-26
4.			PROCESS MODELING	(27-33)
	4.1.		Computational Approach using MAT LAB Coding	28
	4.2.		Model equations	29-30
	4.3.		Results and Discussion	31-33
		4.3.1	Effect of velocity on rate constant	31
		4.3.2.	Effect of bed height on conversion	31-32
		4.3.3.	Effect of time on conversion	32-33
		4.3.4.	Effect of conversion on selectivity	32-33
5.			OBSERVATION AND RESULTS	(34-44)
	5.1.		Preliminary analysis of biomass samples	35-38
		5.1.1.	Ultimate analysis	35
		5.1.2.	Thermo gravimetric Analysis	35-36
		5.1.3.	Proximate analysis	35-36

	5.1.4.	Analysis other properties	36-38
5.2.		Calculation of chemical formulas of the biomass samples	38-39
5.3.		Experimental results for cold model unit	40-43
5.4.		Experimental results for cold model unit	43-44
6.		DISCUSSION AND CONCLUSION	(45-55)
6.1.		Cold model	46-54
	6.1.1.	Effects of individual system parameters on ER	47-49
	6.1.2.	Effects of individual system parameters on Eu	50-52
6.2.		Hot model	54
6.3.		Conclusion	54-55
6.4.		Scope of the work	55
		NOMENCLATURE	(56-58)
		REFERENCES	(59-62)
		APPENDIX	(63-66)

LIST OF FIGURES

Sl. no.	Fig. no.	Title	Page no.
1.	Fig-2.1	Schematic diagram of fluidized bed reactor	7
2.	Fig-2.2	Thermodynamically stable states of calcium sulphate at atmospheric pressure	10
3.	Fig-2.3	Diagrammatic representation of high temperature fluidized bed reactor used in preparation of carbonaceous adsorbents	12
4.	Fig-2.4	Formation and reduction of NO and N_2O during combustion of coal	13
5.	Fig-2.5	Schematic of process flow diagram of fluorination reaction in a FBR	14
6.	Fig-2.6	Schematic diagram of pyrolysis and gasification process in a fluidized-bed reactor	15
7.	Fig-2.7	A typical three layer Neural Network	16
8.	Fig-2.8	Fluidized bed reactor geometry and boundary conditions	17
9.	Fig-2.9	Biomass gasification basics	18
10.	Fig-3.1	Experimental set-up of a cold model fluidized bed gasifier	23
11.	Fig-3.2	Laboratory set-up of a cold model fluidized bed gasifier	23
12.	Fig-3.3	Experimental set-up of a hot model fluidized bed gasifier	25
13.	Fig-3.4	Laboratory set-up of a hot model fluidized bed gasifier	26
14.	Fig-4.1	Graphical abstract of a fluidized bed reactor	28
15.	Fig-4.2	Plot of rate constant versus Velocity	31
16.	Fig-4.3	Plot of conversion versus Bed height	32
17.	Fig-4.4	Plot of conversion versus Time	33
18.	Fig-4.5	Plot of selectivity versus Conversion	33
19.	Fig-5.1	Results of TGA for different biomass samples	36

20	Fig-5.2	Correlation plot of experimental values of ER against the system parameters	41
21.	Fig-5.3	Correlation plot of experimental values of Eu against the system parameters	42
22.	Fig-5.4(a)	Comparison of calculated values of equivalence ratio obtained from Dimensionless analysis against the experimental ones	42
23.	Fig-5.4(b)	Comparison of calculated values of Euler's number obtained from Dimensionless analysis against the experimental ones	43
23.	Fig-6.1	Effect of individual system parameters on ER	47
24.	Fig-6.2	Effects of static bed height on Equivalence ratio	48
25.	Fig-6.3	Effects of particle diameter on Equivalence ratio	48
26.	Fig-6.4	Effects of particle density on Equivalence ratio	49
27.	Fig-6.5	Effects of particle density on Equivalence ratio	50
28.	Fig-6.6	Effects of static bed height on Euler's number	51
29.	Fig-6.7	Effects of particle diameter on Euler's number	51
30.	Fig-6.8	Effects of particle density on Euler's number	52

LISTS OF TABLES

Sl. no.	Table no.	Title	Page no.
1.	3.1	Scope of the experiment	24
2.	5.1	Results of Ultimate Analysis	35
3.	5.2	Results of Proximate Analysis for different biomass samples	36
4.	5.3	Data on other properties for different biomass samples	38
5.	5.4	Chemical formulas of biomass samples	39
6.	5.5	Comparison between calculated and experimental values of ER	40
7.	5.6	Comparison between calculated and experimental values of Eu	41
8.	5.7	Product gas composition from the hot model experiment	44
9.	6.1	Comparison of calculated values of the ER and Eu using MAT LAB and the experimental values.	53
10.	6.2	Percentage deviations of the calculated values of the ER and Eu from the experimentally observed values and chi square values for the correlation-fit.	54

ABSTRACT

The effect of different system parameters (viz. static bed height, fluidization velocity, reaction time etc.) on reaction kinetics which affects the conversion or yield of product in a fluidized bed reactor has been studied. The graphical abstract of the reactor has been drawn. The MAT LAB coding has been developed based on the data of the reactor system. With the help of this coding, the effect of variation of time, bed height and flow rate on conversion and rate constant has been observed.

The behaviour of the cold-model fluidized bed gasifier unit has been studied by considering the different system parameters (viz. H_s, d_p, ρ_s). Experiments were carried out using a Perspex column of 15cm and 30 cm inside diameter for the dense and free board section respectively. Column height is selected as 195cm. Attempts have been made to develop correlations for the Equivalence Ratio and Euler's number by varying different system parameters on the basis of dimensionless analysis. The Equivalence Ratio and Euler's number were also calculated through the MAT LAB programming. The calculated values of the Equivalence Ratio and Euler's number obtained through the dimensionless analysis and MAT LAB programming have been compared with the experimentally measured values for which the percentage of deviations are found to be well within the allowable limits indicating a very good approximation. Comparison of calculated values of Equivalence ratio and Euler's number with the experimentally observed values of the same gives the standard deviations to be 1.89% and 10.8% respectively. Chi-square (ξ^2) test gives 0.0002 and 18685.04 for Equivalence Ratio and Euler's number respectively indicating the correlation fit to be satisfactory. Thus it can be concluded that these developed correlations can be applied over a wide range of parameters for the industrial uses and for the pilot plant unit with a suitable scale-up factor. The carbon conversion efficiency of the hot-model fluidized bed gasifier unit is found out to be 81.7% using saw dust as the biomass material.

***Key- words*:** Fluidized bed reactor, Fluidized bed gasifier, Equivalence ratio, Euler's number, Chi-square (ξ^2), Standard deviation, Mean deviation, Dimensionless Analysis, MAT LAB Coding.

THESIS-SYNOPSIS

The effect of Parameters on the performance of a Fluidized Bed Reactor and Gasifier

The effect of the parameters on reaction kinetics has been studied for the fluidized bed reactor. Fluidized bed Gasifier has been used for gasification of biomass samples. A general simulation has been done by using the MAT LAB coding for the catalytic reaction.

In any reactor, the system parameters like static bed height, gas flow rate, residence time etc. affect the rate of a reaction thereby affecting the conversion or the yield of the operation. Therefore attempt has been made to develop a generalized standard model for a fluidized bed reactor which will be of a great use for industrial practices. It has also been planned to validate the developed model with the experimental data.

The present work for M. Tech. thesis has been presented in six chapters.

Chapter-1 (Introduction) :

The chapter-1 deals with the introduction regarding the fluidized bed reactor and reason for using the process simulation software like MAT LAB coding. Process simulation software describes processes in flow diagrams where unit operations are positioned and connected by product or educts streams. The software has to solve the mass and energy balance to find a stable operating point. The goal of a process simulation is to find optimal conditions for an examined process. This is essentially an optimization problem which has to be solved in an iterative process. The present work is based on the study of the effect of various systems parameters on reaction kinetics in a fluidized bed reactor which affects the conversion or yield of product. Although some basic formulas for fluidized bed reactors are already developed by some researchers but the detail kinetic studies of the reactor with varying system parameters are required to be investigated and the attempt has been made for mathematical modeling. The graphical abstract of the reactor has been drawn and the MAT LAB coding has been developed based on the data of the reactor system. With the help of this coding, the effect of different system parameters on conversion and rate constant has been observed which have been shown by different plots. In the present work attempt has also been made to study the gasification processes of the biomass

samples in the fluidized bed reactor. The co-relations for the equivalence ratio and Euler's number have also been developed for the cold model experimental set-up. The carbon conversion efficiency of the hot model experiment was also found out by considering the saw dust as the biomass sample.

Chapter-2 (Literature Survey) :

Chapter-2 deals with the literature surveys on the fluidized bed reactor in which the working principles, applications and research works of various authors are discussed.

Kinetic study of Colorado oil shale pyrolysis in a fluidized-bed reactor had been carried out by a group of investigators [1]. Again some researchers [2] had tried to remove fluoride from industrial wastewaters by crystallization process in a fluidized bed reactor in order to decrease the sludge formation as well as to recover fluoride as synthetic calcium fluoride.

Some more investigators [3] carried out experiments for the rate of dehydration of desulphurized gypsum mm and at bed temperatures of 100 to 1708 ℃ in a fluidized bed reactor. The kinetics of reaction of the uranium tetra fluoride conversion to the uranium hexafluoride has also been studied with fluorine gas in a fluidized bed reactor operating in industrial conditions [4]. The effect of secondary fluidizing medium on bed pressure drop, fluctuation and expansion ratios in a cylindrical gas–solid fluidized bed using Artificial neural network (ANN) and factorial design (statistical approach) models had also been studied [5]. A new mechanism and kinetics model for di-methyl ether (DME) synthesis has also been established in a laboratory scale fluidized-bed reactor [6].

Chapter-3 (Experimentation) :

Chapter-3 deals with the experimental work carried out in the cold model and hot model of a laboratory unit fluidized bed gasifier. Various types of raw materials such as saw dust, rice husk, rice straw and mixed biomass have been used for the experimental work. Some preliminary analysis of the biomass samples were carried out before the experimental work which involves determination of bulk density, mean particle diameter, sphericity and porosity. The chemical formulas of the biomasses were also found out by the ultimate analysis of the biomass samples. Then the experiment was carried out in the cold model section of the laboratory unit fluidized

bed gasifier. The different system parameters like the static bed height, particle diameter, particle density were varied during the experimentation to study their effects on pressure drop and thereby on the equivalence ratios. Various parameters under study are listed in the scope of the experiment (Table-1). The experiment was then carried out in the hot model by using the saw dust as the raw materials. The chars obtained from the hot model experiment were analyzed to know the carbon percentage by the ultimate analysis.

Table-1: (Scope of the experiment)

Materials	**H_s (cm)**	**d_p (mm)**	**ρ_s (kg/m^3)**
Silica	2.5	1.65	1602
Silica	3.0	1.65	1602
Silica	4.5	1.65	1602
Dolomite	6.5	1.65	1602
Dolomite	4.5	2.25	1602
Dolomite	4.5	1.65	1602
Calcium carbide	4.5	1.2	1602
Calcium carbide	4.5	0.75	1602
Calcium carbide	4.5	1.65	1602
Al balls	4.5	1.65	2940
Al balls	4.5	1.65	1201
Al balls	4.5	1.65	2700

Chapter-4 (Simulation Modeling using MATLAB) :

Chapter-4 comprises the process modeling part in which MAT LAB coding was developed. This typically involves use of MAT LAB simulation software to define a system which is solved so that the steady-state or dynamic behavior can be predicted. The system components and connections are represented as a Process Flow diagram. The graphical abstract of a fluidized bed reactor is as shown in Figure-1 and the MATLAB coding has been developed by considering the different system parameters. A number of modeled equations were used for the design of the fluidized bed reactor. By using the values of the above mentioned parameters, the programme was run and the effects of the parameters on reaction kinetics were observed which are discussed by different plots in the main thesis such as, velocity versus rate constant, height versus conversion, time versus conversion and conversion versus selectivity.

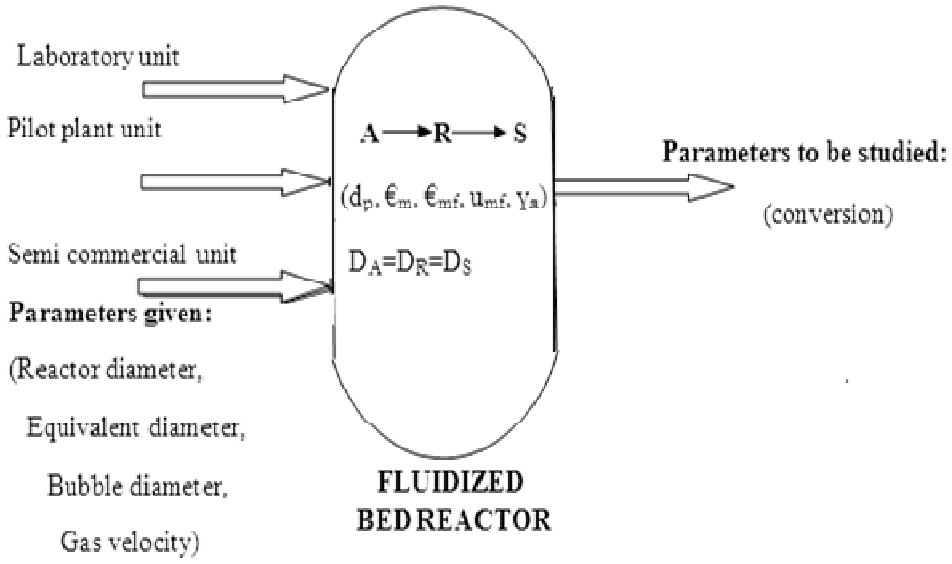

Figure–1: Graphical abstract of a fluidized bed reactor

Chapter-5 (Results and Discussion) :

The experimental results and discussion are described in chapter-5. Here the effects of various parameters are shown. The effects of different parameters on reaction kinetics are represented by individual plots for the parameters, the co-relation plots and the result tables. The results for Equivalence Ratio (ER) and Euler's number (Eu) have been represented in the following generalized equations.

$$ER = K\left[\left(\frac{H_s}{D_c}\right)^a\left(\frac{d_p}{D_c}\right)^b\left(\frac{\rho_s}{\rho_f}\right)^c\right]^n \quad (1)$$

$$Eu = K'\left[\left(\frac{H_s}{D_c}\right)^{a'}\left(\frac{d_p}{D_c}\right)^{b'}\left(\frac{\rho_s}{\rho_f}\right)^{c'}\right]^{n'} \quad (2)$$

Final results are thus discussed with the justifications. It has been planned to compare the theoretical result against the experimental ones.

Chapter-6 (Conclusion) :

Finally the work has been concluded with a good result in Chapter-6. From both theoretical and experimental results it is observed that the system parameters play a vital role in the optimum design of a fluidized bed reactor. Thus the present work of laboratory level can be suitably modified over a wide range of parameters for a commercial or large scale fluidized bed reactor.

Nomenclature :

H_s : Static bed height, cm

D_c : Diameter of the fluidized bed column, cm

d_p : Particle size, mm

ρ_s : Density of the solid particle, kg/m^3

ρ_f : Density of air, kg/m^3

ER : Equivalence ratio, dimensionless

Eu : Euler's number, dimensionless

References :

[1] Braun, R. L. and Burnham, A. K., (1985), kinetics of Colorado fluidized-bed reactor oil, Lawrence Livermore National Laboratory, Livermore, CA 94550, USA.

[2] Aldaco, R., Garea, A. and Irabien, A., Particle growth kinetics of calcium fluoride in a fluidized bed reactor, (2007), Chemical Engineering Science 62: (2958-2966).

[3] Cave, S. R. and Holdich, R.G., (2000), the hydration kinetics of gypsum in a fluidized bed reactor, Institution of Chemical Engineers Trans IChemE, Vol 78, Part A.

[4] Khani, M. H., Pahlavanzadeh, H., Ghannadi, M., (2008), kinetics study of the fluorination of uranium tetra fluoride in a fluidized bed reactor, Annals of nuclear energy 35: (704-707).

[5] Mohanty, Y. K., Mohanty, B. P., Roy, G. K. and Biswal, K. C., (2009), effect of secondary fluidizing medium on hydrodynamics of gas-solid fluidized bed- statistical and ANN approaches, Chemical Engineering Journal 148: (41-49).

[6] Papadikis, K., Gu, S. and Bridgwater, A. V., (2010), computational modeling of the impact of particle size to the heat transfer coefficient between biomass particles and a fluidized bed, Fuel processing technology 91: (68-79).

CHAPTER-1

INTRODUCTION

Introduction

The study of the reaction kinetics is very much important during the design of the fluidized bed reactor. With the help of this study one can know how the parameters like static bed height, gas flow rate, residence time etc. affect the rate of a reaction thereby percentage of conversion of the reactants for the optimum design. The rate of a chemical reaction is a measure of variation of the concentration or pressure of the involved substances with time. Analysis of reaction rates is therefore important for several applications in chemical engineering or in chemical equilibrium studies.

1.1. IMPORTANT FACTORS TO STUDY FOR THE REACTION KINETICS OF A PROCESS

Rates of reaction depend basically on the following factors.

- Reactant concentrations; which usually make the reaction happen at a faster rate if raised through increased collisions per unit time,
- Available surface; exposed surface area of particles for contact between the reactants increases in particular in heterogeneous systems of solid ones. Larger surface area leads to higher reaction rates.
- Pressure within the system; by increasing the pressure, volume between the molecules decreases which increases the frequency of collisions among molecules.
- Activation energy; Higher activation energy for a reaction implies that the reactants need more energy to participate in the reaction than the reactants of a reaction with lower activation energy.
- Temperature; which hastens reaction rates if raised thereby creating more collisions per unit time. This is so because higher temperature increases the energy of the molecules,
- The presence or absence of a catalyst; which change the pathway (mechanism) of a reaction thereby increasing the speed of a reaction by lowering the activation energy needed for the reaction to take place. A catalyst is not destroyed or changed during a reaction; as a result it can be re-used.
- For some reactions, the presence of electromagnetic radiation, most notably ultraviolet, is needed to promote the breaking of bonds to start the reaction. This is particularly true for reactions involving radicals.

1.2. PROCESS MODELING

Process simulation is used for the design, development, analysis, and optimization of technical processes and is mainly applied to chemical plants and chemical processes, but also to power stations, and similar technical facilities. Process simulation software describes processes in flow diagrams where unit operations are positioned and connected by product or educts streams. The software has to solve the mass and energy balance to find a stable operating point. The goal of a process simulation is to find optimal conditions for an examined process. This is essentially an optimization problem which has to be solved in an iterative process.

A fluidized bed reactor (FBR) is a type of reactor device that can be used to carry out a variety of multiphase chemical reactions. In this type of reactor, a fluid (gas or liquid) is passed through a granular solid material (usually a catalyst possibly shaped as tiny spheres) at high enough velocities to suspend the solid and cause it to behave as though it were a fluid. This process, known as fluidization, imparts many important advantages to the FBR. As a result, the fluidized bed reactor is now used in many industrial applications.

The first fluidized bed gas generator was developed by Fritz Winkler in Germany in the 1920s. The principle behind this is that the solid substrate (the catalytic material upon which chemical species react) material in the fluidized bed reactor is typically supported by a porous plate, known as a distributor.

1.3. APPLICATIONS OF FLUIDIZED BED REACTOR

Today fluidized bed reactors are still used to produce gasoline and other fuels, along with many other chemicals. Many industrially produced polymers are made using FBR technology, such as rubber, vinyl chloride, polyethylene, and styrenes. Various utilities also use FBR's for coal gasification, nuclear power plants, and water and waste treatment settings. Used in these applications, fluidized bed reactors allow for a cleaner, more efficient process than previous standard reactor technologies.

1.4. ADVANTAGES OF FLUIDIZED BED REACTOR

The increase in fluidized bed reactor use in today's industrial world is largely due to the inherent advantages of the technology.

- Due to the intrinsic fluid-like behavior of the solid material, fluidized beds do not experience poor mixing as in packed beds. This complete mixing allows for a uniform product that can often be hard to achieve in other reactor designs. The elimination of radial and axial concentration gradients also allows for better fluid-solid contact, which is essential for reaction efficiency and quality.
- Many chemical reactions require the addition or removal of heat. Local hot or cold spots within the reaction bed, often a problem in packed beds, are avoided in a fluidized situation such as an FBR. In other reactor types, these local temperature differences, especially hotspots, can result in product degradation. Thus FBRs are well suited to exothermic reactions. Researchers have also learned that the bed-to-surface heat transfer coefficients for FBRs are high.
- The fluidized bed nature of these reactors allows for the ability to continuously withdraw product and introduce new reactants into the reaction vessel. Operating at a continuous process state allows manufacturers to produce their various products more efficiently due to the removal of startup conditions in batch processes.

The present work is based on the study of the effect of various systems parameters on reaction kinetics in a fluidized bed reactor which affects the conversion or yield of product. Although some basic formulas for fluidized bed reactors are already developed by some researchers but the detail kinetic studies of the reactor with varying system parameters are required to be investigated and the attempt has been made for mathematical modeling. The graphical abstract of the reactor has been drawn and the MAT LAB coding has been developed based on the data of the reactor system. By the help of this coding, the variation of time, bed height and flow rate on conversion and rate constant has been observed which have been shown by different plots. In the present work attempt has also been made to study the gasification processes of the biomass samples in the fluidized bed reactor. The correlation of the equivalence ratio and Euler's number has also been developed for the cold model experimental set-up and the carbon conversion efficiency of the hot model experiment was found out by taking the saw dust as the raw material. The Standard deviation, Mean deviation and Chi-square (ξ^2) tests were done for Equivalence ratio and Euler's number to known whether the correlation fits to be satisfactory or not.

1.5. OBJECTIVE OF THE WORK

1.5.1. Experimental:

- To develop the correlation for the Equivalence ratio and the Euler's number for a cold-model fluidized bed gasification unit and thereby to compare the effect of individual system parameters (viz. static bed height, particle diameter, particle density etc.) on the same.
- To find out the properties of the biomass samples by carrying out some preliminary analysis (viz. Ultimate analysis, Proximate analysis, T.G. Analysis etc.).
- To find out the equivalence ratio and carbon conversion efficiency of the biomass samples in a Hot-model gasifier unit.

1.5.2. Computational:

- A MAT LAB coding has been developed for the catalytic fluidized bed reactor to know the effects of parameters like static bed height, residence time etc. on reaction kinetics.
- MAT LAB coding has also been developed to calculate the values of Equivalence ratio and Euler's number and thereby to compare with the experimentally observed values.

CHAPTER-2

LITERATURE SURVEYS

One of the first United States fluidized bed reactors used in the petroleum industry was the Catalytic Cracking Unit. This FBR and the many to follow were developed for the oil and petrochemical industries. Here catalysts were used to reduce petroleum to simpler compounds through a process known as cracking. The invention of this technology made it possible to significantly increase the production of various fuels in the United States.

2.1. PRINCIPLES OF FLUIDIZED BED REACTOR

The solid substrate (the catalytic material upon which chemical species react) material in the fluidized bed reactor is typically supported by a porous plate, known as a distributor. The fluid is then forced through the distributor up through the solid material. At lower fluid velocities, the solids remain in place as the fluid passes through the voids in the material. This is known as a packed bed reactor. As the fluid velocity is increased, the reactor will reach a stage where the force of the fluid on the solids is enough to balance the weight of the solid material. This stage is known as incipient fluidization and occurs at this minimum fluidization velocity. Once this minimum velocity is surpassed, the contents of the reactor bed begin to expand and swirl around much like an agitated tank or boiling pot of water. The reactor is now a fluidized bed. Depending on the operating conditions and properties of solid phase various flow regimes can be observed in this reactor [1].

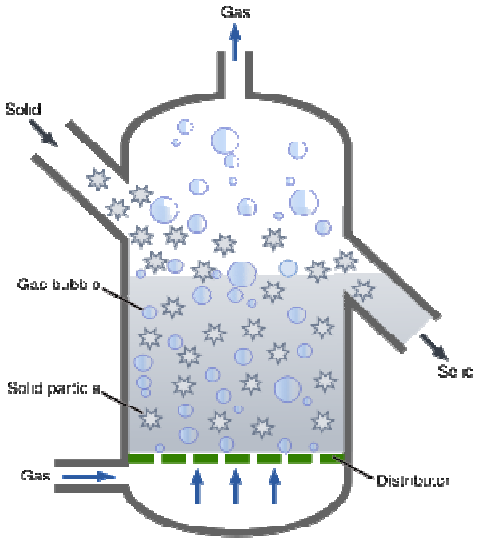

Figure–2.1: Schematic diagram of fluidized bed reactor [1]

The behaviour of fluidized bed reactor at its fully developed stage requires the understanding of particles-fluid motion at the beginning of and after fluidization. It is experimentally well known that the pressure drop across the bed after fluidization could be described by Carman-Kozeny equation [2]. When the fluid velocity has reached minimum fluidized one, the pressure drop across the bed will be equal to the total weight of the constituent particles per unit area. At the moment of minimum fluidization or the onset of particles motion, the net gravitational force acting downwards on each particle is balanced by the upwards component of the drag force. In order to ascertain the physical validity of Froude number as the criterion for prediction, it is required to consider the particles motion from their initial contact to onset of minimum fluidization.

2.2. PREVIOUS WORKS

Kinetic study of Colorado oil shale pyrolysis in a fluidized-bed reactor had been done by a group of authors [3]. It has been observed that the rate expressions were independent of shale source and particle size (0.5-2.4 mm). They concluded that the small incremental oil yield possible for Fluidized-bed pyrolysis requires a longer residence time than that estimated by kinetic expressions derived from slow-heating data.

The effects of kinetics, hydrodynamics and feed conditions on methane coupling using fluidized bed reactor has been studied by Al-Zahrani et. al [4]. Bubbling fluidized bed reactors have been used in the investigation to observe the effect of above parameters. The simulation results revealed that increasing the ratio of methane to oxygen in the feed leads to lower methane conversion but higher C_2 selectivity. Higher methane conversion and product selectivity are obtained upon decreasing the feed flow rate and particle diameter. Oscillatory operation has been found to occur the amount of methane in the feed is decreased.

Attempts had been done for Crystallization process to remove fluoride from industrial wastewaters in a fluidized bed reactor in order to decrease the sludge formation as well as to recover fluoride as synthetic calcium fluoride. Removal of fluoride by crystallization process in a fluidized bed reactor using granular calcite as seed material has been carried out in a laboratory-scale fluidized bed reactor in order to study the particle growth kinetics for modeling, design, control and operation purposes. The main variables have been studied, including superficial velocity (SV, ms^{-1}), particle size of the seed material (L_0, m) and super saturation (S). It has been

developed a growth model based on the aggregation and molecular growth mechanisms. The kinetic model and parameters given by the equation [5]:

$$G = (2.26 \times 10^{-10} + 2.82 \times 10^{-3} L_0^{\,2}) S V^{0.5} S \qquad (2.1)$$

Benzene ethylation has been investigated over fresh ZSM-5 based catalyst in a riser simulator that mimics the operation of a fluidized-bed reactor [6]. Experimental runs for the kinetic study were carried out at four different temperatures (300, 325, 350 and 400 °C) for reaction times of 3, 5, 7, 10, 13, and 15 s. Benzene to ethanol (B/E) mole ratio was varied from 1:1 to 3:1. Benzene conversion, ethyl benzene yield and diethyl benzene yield were found to increase with reaction temperature and time. The maximum benzene conversion of 16.95% in which the main products were ethyl benzene.

The CO_2 reforming of methane to synthesis gas over an Ni (1 wt %) /a-Al_2O_3catalyst was also been studied in lab-scale fluidized-bed reactors (ID=3,5 cm) [7]. Highest conversions and syngas yields were achieved applying the following reaction conditions: TR=800^{o}C, H_{mf}=5 cm, u/u_{mf}=11.8, p_{CH4}: p_{CO2}:p_{N2}= 1: 1: 2. Methane and carbon dioxide conversion amounted to 90 and 93%, respectively. Hydrogen and carbon monoxide yield amounted to 81 and 90%, respectively; this corresponds to a H_2: CO ratio of 0.9.

Combustion studies with metallurgical cokes have also been carried out in batch experiments in an electrically heated fluidized bed reactor. Different experiments were carried out in air at temperatures ranging from 750 ℃ to 950 ℃ and coke diameters between 0.675 to 3.500 mm. The overall rate constant at each burn off stage were obtained. The dependence of chemical rate constant on temperature can be described by equation [8]:

$$K_p[kg/(cm^2\ s\ atmo_2)] = 30 \exp(-22{,}340/RT_p) \qquad (2.2)$$

The performance of a pilot scale fluidized bed membrane reactor (FLBMR) had been studied experimentally in comparison to the conventional operation as a fluidized bed reactor (FLBR) for the catalytic oxidative dehydrogenation of ethane using a g-alumina supported vanadium oxide catalyst [9]. The influence of process parameters such as temperature and contact time, for both reactor configurations has also been investigated. Further, the experimental data obtained were compared to previous experiments with a fixed-bed reactor (FBR) and a packed-bed

membrane reactor (PBMR) operated with a similar catalyst. Ethylene is one of the most important raw materials in the industrial organic chemistry. Ethylene is widely applied in important technical processes for the production of other valuable base chemicals, e.g. polyethylene and copolymers, ethylene oxide, acetaldehyde, ethanol, vinyl acetate, and higher linear olefins and alcohols [10]. It is the feedstock near 30% of all produced petrochemicals [11]. The FLBMR concept combines the excellent heat transfer properties of fluidized beds with the advantages of a distributed oxidant dosing, both having a beneficial effect on the reactor performance. Finally, it has been demonstrated, that the use of metallic instead of ceramic membranes helps to overcome the sealing problems in the field of constructing membrane reactors. Thus, the fluidized bed membrane reactor concept appears to be very attractive for industrially important exothermic reactions where selectivity to the intermediate product is of prime importance, like for the selective oxidation of hydrocarbons.

Experiments have been carried out for the rate of dehydration of desulphurized gypsum with particle diameters in the range of (35±67) mm and at bed temperatures of 100 to 1708^{o}C in a fluidized bed reactor [12]. The fluidizing gases were air, with water vapor pressures of the range of 0.001 to 0.35 atmosphere, and carbon dioxide. It has been found out that the reaction rate was increased with increasing temperature, decreasing particle size, decreasing water vapor pressure with suppression of the hemihydrates to anhydrite reaction at high water vapor pressures, decreasing air pressure. Kelly [13] provided a thermodynamic analysis of the various states of gypsum dehydration, under different conditions of water vapor pressure and temperature, and that was shown in Figure-2.2.

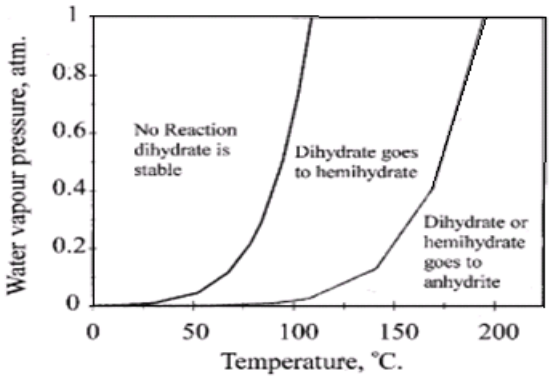

Figure-2.2: Thermodynamically stable states of calcium sulphate at atmospheric pressure.

The decomposition kinetics has been studied by many investigators. There is no consensus on the mechanism. Mass transfer, heat transfer, chemical kinetics, and combinations of these have all been reported as rate limiting. In general, the reaction rate has been found to increase with:

- Increasing temperature [14-18];
- Decreasing particle size [15, 16, 19];
- Decreasing water vapor pressure [20] with suppression of the hemihydrates to anhydrite reaction at high water vapor pressures [21];
- Decreasing air pressure [22] to a maximum rate at 1mm Hg.

A group of authors were carried out experiments with eight different chars in a batch fluidized bed reactors. The combustion rate was determined by measuring the co and co_2 concentrations in the flue gas. Four models were tested, but only two well described the combustion rates for all tested chars. The effect of temperature and particle size on the combustion rate and the rate controlling step were determined. Arrhenius equation provides the apparent activation energy and the pre-exponential factor [23]. The experiments were extended to larger particle size and the temperature dependence of the reaction rate constant was analyzed.

The fluidized bed reactor can also be utilized for the production of adsorbents in removal of malachite green. Activation carbon was prepared from rubber wood sawdust by steam and chemical treatments. Steam activation was carried out in high temperature fluidized bed reactor (FBR) using steam as quenching medium. Chemical activation was carried out by using phosphoric acid. The adsorption capacity was determined by using iodine number and methylene blue number and surface area by ethylene glycol mono ethyl ether (EGME) method. Further the adsorption studies were carried out using malachite green dye. Langmuir, Freundlich and Temkin adsorption isotherms were analyzed and Langmuir isotherm shows satisfactory fit to experimental data. The adsorption capacity was found to decrease in the order; steam activated carbon > acid + steam activated carbon > commercial activated carbon > acid activated carbon. Temperature effects on adsorption were carried out and it was found that the adsorption reaction was endothermic. The adsorption kinetics was found to follow pseudo-second-order kinetic model [24].

Activated carbon was prepared using steam activation in a FBR as well as chemical activation in a packed bed reactor as well as in a FBR. The diagrammatic representation of the FBR is given in Figure-2.3.

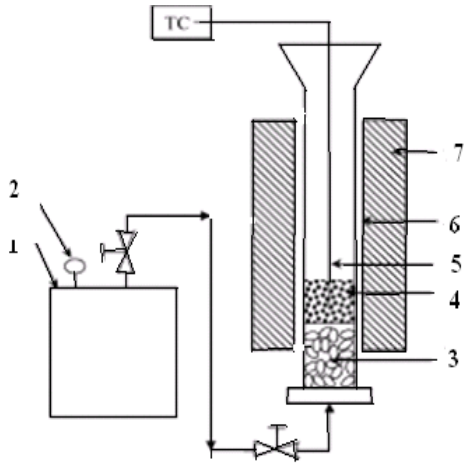

1.	Steam generator	5.	Thermocouple
2.	Pressure gauge	6.	Fluidized bed reactor
3.	Ceramic beads	7.	Electric heater
4.	Carbon		

Figure-2.3: Diagrammatic representation of high temperature fluidized bed reactor used in preparation of carbonaceous adsorbents.

The changes in enthalpy (δH°), entropy (δS°) and the freeenergy (δG°) were evaluated using the equations given below [25]:

$$\delta G^\circ = - RT \ln b \quad (2.3)$$

$$\ln\left(\frac{b_2}{b_1}\right) = -\frac{\delta H^o}{R}\left(\frac{1}{T_1} - \frac{1}{T_2}\right) \quad (2.4)$$

$$\delta S^o = \left(\frac{\delta G^o - \delta H^o}{T}\right) \quad (2.5)$$

Li et. al [26] presented a comprehensive and critical review of the mechanisms and kinetics of NO and N_2O reduction reaction with coal chars under fluidized bed combustions (FBC). Important kinetic factors such as the rate expressions, kinetics parameters as well as the effect of surface area and pore structure are discussed in detail. The main factors influencing the reduction of NO and N_2O in FBC conditions are the chemical and physical properties of chars and the

operating parameters of FBC such as temperature, presence of CO, O_2 and pressure. It is generally believed that the amount of NO and N_2O emitted from fluidized bed combustors is the result of homogeneous and heterogeneous formation and in situ destruction reactions. A schematic representation of NO, N_2O formation and reduction in FBC in figure-2.4.

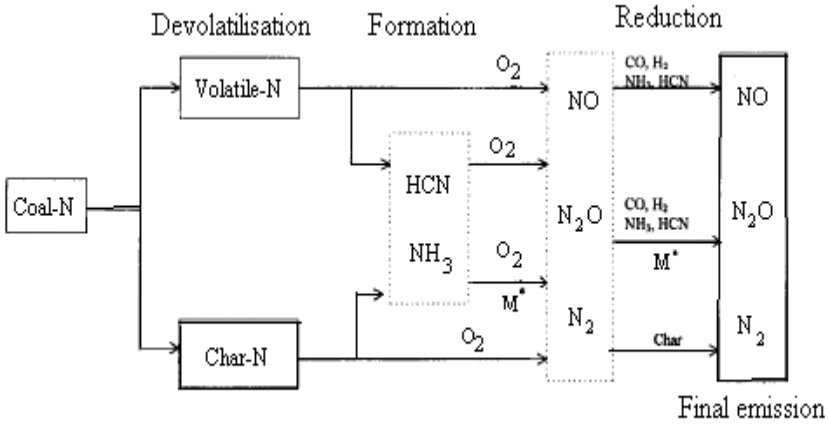

Where **M***= Catalyst (char. limestone, ash and bed materials)

Figure-2.4: Formation and reduction of NO and N_2O during combustion of coal

The kinetics of reaction of the uranium tetra fluoride conversion to the uranium hexafluoride has also been studied with fluorine gas in a fluidized bed reactor operating in industrial conditions [27]. The external and internal diffusion effects are investigated by Mears and Weisz–Prater criterions. The kinetic equation for the fluorination of uranium tetra fluoride is developed in the absence of diffusional limitation using an integral method by assuming that the gas flow is of plug or perfectly mixed type. A good agreement is observed between the experimental data and a first-order model with respect to fluorine in the CSTR system. The activation energy of the reaction and the pre-exponential factor are obtained using analytical results. Uranium hexafluoride is a very important chemical product in the production of nuclear fuel. Natural Uranium hexafluoride in industrial production is mainly used as the raw material in the uranium enrichment plant. The fluorination reaction is:

$$UF_4 + F_2 = UF_6 \qquad (2.6)$$

Fluorination data were collected from the fluidized bed reactor. Fig-2.5 illustrates the essential features of this process.

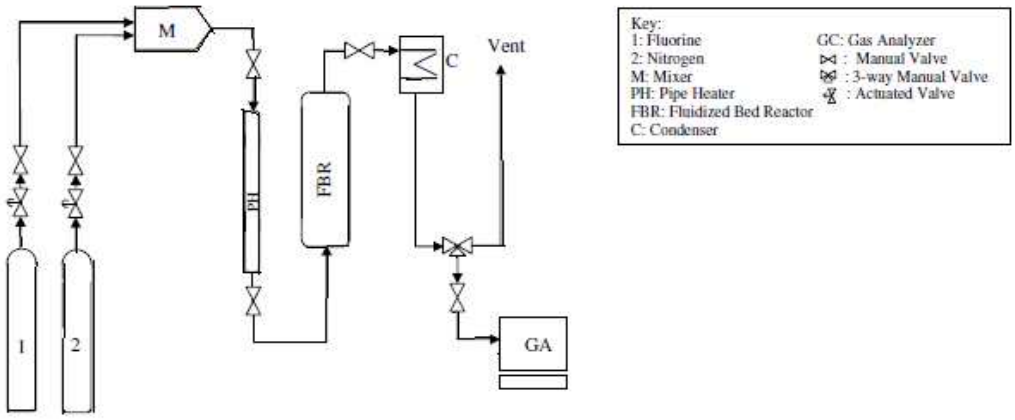

Figure-2.5: Schematic of process flow diagram of fluorination reaction in a FBR

Attempts had also been carried out by a group of scientists for Coal pyrolysis and gasification reactions in a fluidized-bed reactor (0.1 m internal diameter by 1.6 m height) over a temperature range from 1023 to 1173 K at atmospheric pressure [28]. The overall gasification kinetics for the steam–char and oxygen–char reactions was determined in a thermo balance reactor. It has been observed that the heating value increases with increasing temperature and steam/coal ratio but decreases with increasing air/coal ratio. Coal gasification with O_2 and H_2O in a fluidized-bed reactor involves pyrolysis, combustion and steam gasification. Pyrolysis and gasification carried out in a fluidized-bed reactor (316 stainless steel) are as shown in figure-2.6.

With a view of exploiting renewable biomass energy as a highly efficient and clean energy, liquid fuel from biomass pyrolysis, called bio-oil, is expected to play a major role in future energy supply. At present, fluidized bed technology appears to have maximum potential in producing high-quality bio-oil [29]. A model of wood pyrolysis in a fluidized bed reactor has been developed. The model shows that reaction temperature plays a major important role in wood pyrolysis. It was shown that particles less than 500 μm could achieve a high heating- up rate to meet flash pyrolysis demand.

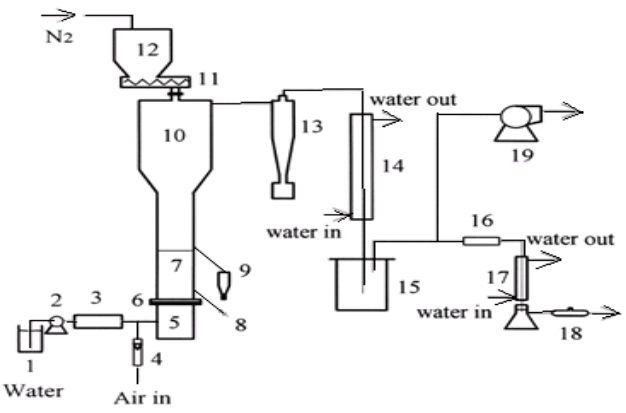

1.	Water reservoir	11.	Screw feeder
2.	Master pump	12.	Coal hopper
3.	Steam generator	13.	Cyclone
4.	Air flow meter	14.	Condenser
5.	Air box	15.	Collector
6.	Distributor	16.	Dust filter
7.	Main bed	17.	Condenser
8.	Bed drain	18.	Gas sampling bottle
9.	Overflow	19.	I.D. fan
10.	Free board		

Figure-2.6: Schematic diagram of pyrolysis and gasification process in a fluidized-bed reactor

A fluidized-bed photo catalytic reactor had also been used for water pollution abatement by Chiovettaet. al [30]. A mathematical scheme is developed to analyze the fluidized bed, including a detailed radiation field representation and an intrinsic kinetic scheme. The model is used to predict operating conditions at which good mixing states and fluid renewal rates are accomplished throughout the bed, and to compute contaminant decay. For relatively high flow rates, per-pass oxidation conversions between 9 and 35% are reached depending on the reactor system considered, and on the titanium oxide concentration in the bed, ranging between 0.1 and 0.5 kg m^{-3}. Results indicate a strong dependence of reactor performance upon the radiation energy available at each point in the annulus. For the selected contaminant, the kinetic scheme shows that the low-energy disadvantage in the low-pressure lamp reactor can be compensated by the fact that the radiation field is more evenly distributed throughout the fluidized particle bed.

The effect of secondary fluidizing medium on bed pressure drop, fluctuation and expansion ratios in a cylindrical gas–solid fluidized bed using Artificial neural network (ANN) and factorial design (statistical approach) models had been studied by Mohanty et.al [31]. They developed a model to predict how the pressure drop, fluctuation and expansion ratios varies with varying gas flow rates, bed heights, particle sizes and particle densities. The values of pressure drop, fluctuation and expansion ratios predicted by the developed models for primary, and

simultaneous primary and secondary fluidizing media have been found to agree well with the corresponding experimental values. In order to improve the quality of fluidization and to increase its applicability, the fluidizer can be operated in higher velocity ranges. For identical operating parameters, bed fluctuation and expansion ratios increase with an increase in mass velocity with the exception that expansion ratio decreases under simultaneous primary and secondary air supply conditions. Knowledge of fluctuation ratio and bed pressure drop in gas–solid fluidization is of importance in the design of fluidized bed reactors and combustors, specifically for the calculation of bed height. Computing through neural networks is one of the recently growing areas of artificial intelligence. A software package for artificial neural network in Mat Lab has been used for ANN simulation. Atypical three layers, viz., (i) input (I), (ii) hidden (H) and (iii) output (O) have been chosen. Four nodes in the input layer, three neurons in the hidden layer and one node in the output layer have been taken as shown in Figure-2.7.

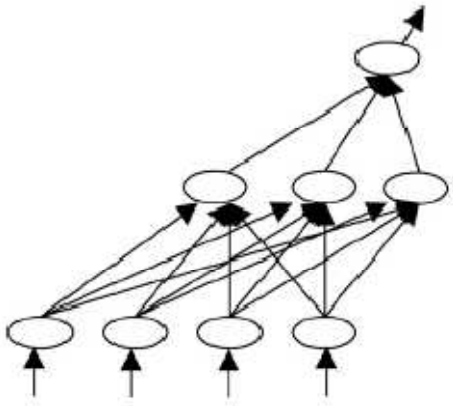

Figure-2.7: A typical three layer Neural Network.

Papadikis et.al [32] were observed the fluid–particle interaction and the impact of different heat transfer conditions on pyrolysis of biomass inside a 150 g/h fluidized bed reactor are modeled. Two different size biomass particles (350μm and 550μm in diameter) are injected into the fluidized bed. The different biomass particle sizes result in different heat transfer conditions. This is due to the fact that the 350μm diameter particle is smaller than the sand particles of the reactor (440μm), while the 550μm one is larger. The bed-to-particle heat transfer for both cases is calculated according to the literature.

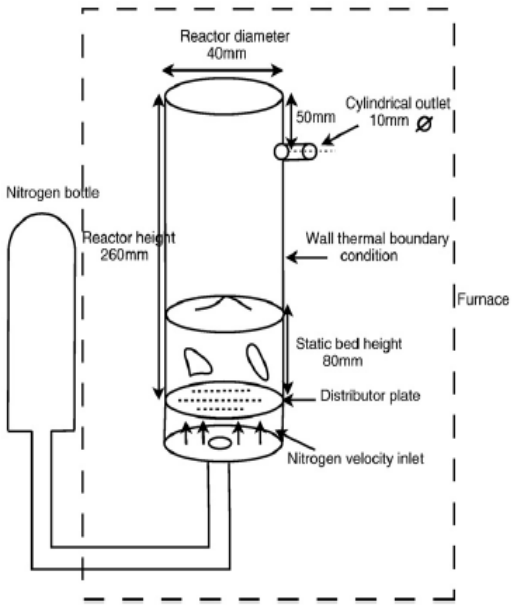

Figure–2.8: Fluidized bed reactor geometry and boundary conditions

The effect of different size particles on the heat transfer coefficient between biomass particles and a fluidized bed was modeled. The results showed that the different size particles which result in different heat transfer mechanism affect the heat transfer coefficient significantly. This results in different temperature profiles at the surfaces and centers of the biomass particles. The temperature gradients inside the particles can be neglected due to their small Biot numbers, which result to uniform radial product distribution at elevated pyrolysis temperatures (>400 °C). The final product yields for different size particles and different heat transfer rates depend on the residence time of the particle in the reactor.

A new mechanism and kinetics model for di-methyl ether (DME) synthesis has also been established in a laboratory scale fluidized-bed reactor [33]. As syngas to dimethyl ether reaction is highly exothermic, fluidized-bed reactor is used because it is highly effective both in heat and mass transfer. Experiments were carried out to assess the performance of DME synthesis in this reactor. Three reactions take place in the syngas-to-DME process, namely,

a. Methanol synthesis reaction:-

   $CO_2 + 3H_2 \Leftrightarrow CH_3OH + H_2O$ (2.7)

   $\delta H = -56.33$ kJ/mol

b. Methanol dehydration reaction:-

$2CH_3OH \Leftrightarrow CH_3OCH_3 + H_2O$ (2.8)

$\delta H = -21.255$ kJ/mol

c. Water gas shift reaction:-

$CO + H_2O \Leftrightarrow H_2 + CO_2$ (2.9)

$\delta H = -40.9$kJ/mol

d. Overall reaction:-

$3CO + 3H_2 \Leftrightarrow CH_3OCH_3 + CO_2$ (2.10)

$\delta H = -256.615$ kJ/mol

The selected catalyst is Cu–ZnO–Al2O3/HZSM-5, manufactured by co-precipitation deposition method with the component for methanol synthesis, Cu–ZnO–Al2O3, and that for methanol dehydration, HZSM-5. The experimental results show that CO conversion and DME productivity are higher than those of fixed bed or slurry reactor.

Gasification reaction can also be done using FBR technology and some literature regarding this taking biomass as the raw materials are as follows:

Gasification is a two step process in which solid fuels (biomass and coal) is thermo chemically converted to a low or medium energy content gas. A highly critical factor in the high energy efficiency of the gasification process is that of the gasifier (primary reformer). The four main gasification stages occur at the same time in different parts of the gasifier as shown in fig.2 below.

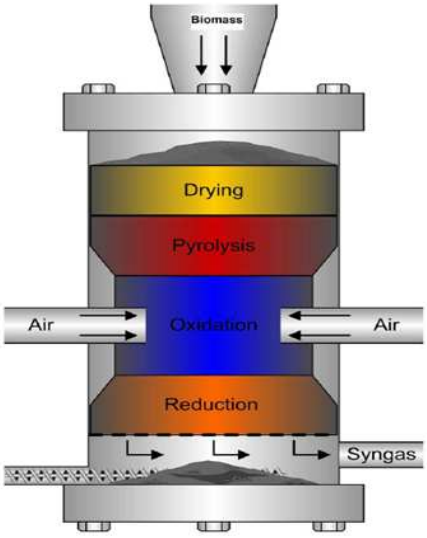

Figure-2.9: Biomass gasification basics

Drying zone:

Biomass fuels consist of moisture ranging from 5 to 35%. At the temperature above 100 °C, the water is removed and converted into steam. Biomass does not experience any kind of decomposition in the drying stage.

Pyrolysis zone:

Pyrolysis is the thermal decomposition of biomass in the absence of oxygen. Pyrolysis involves release of three kinds of products: solid (char), liquid (oil) and gases (CO, H_2, and N). The ratio of products is influenced by the chemical composition of biofuels and operating conditions. The heating value of gas produced during pyrolysis process is low (3.5 to 8.9 MJ/m^3). The dissociated and volatile components of the fuel are vaporized at a temperature of 600^oc or 1100^oF. Hydrocarbon vapors, hydrogen, carbon monoxide, carbon dioxide, tar; water vapors are also included in volatile matters.

Oxidation zone:

The combustion takes place at temperature ranging from 700 to 2000°C. Heterogeneous reaction takes place between oxygen in the air and solid carbonized fuel, producing carbon dioxide as follows.

$$C + O_2 = CO_2 \quad (2.11)$$

Hydrogen in fuel reacts with oxygen in the air blast, producing steam.

$$H_2 + ½\ O_2 = H_2O \quad (2.12)$$

Reduction zone:

In the reduction zone, a number of high temperature chemical reactions take place in the absence of oxygen. The principal reactions that take place are:

$$CO_2 + C = 2CO \quad (2.13)$$

$$C + H_2O = CO + H_2 \quad (2.14)$$

$$CO_2 + H_2 = CO + H_2O \quad (2.15)$$

$$C + 2H_2 = CH_4 \quad (2.16)$$

The main reactions show that heat is required during the reduction process. Hence the temperature of the gas goes down during this stage. If complete gasification takes place, all the carbon is burned or reduced to carbon monoxide, a combustible gas and some mineral matter is vaporized. The remains are ash and char (unburned carbon).

The gases produced in gasification process have the following composition:

Carbon monoxide: - 20-22%

Hydrogen: - 15-18%

Methane: - 2-4%

Carbon dioxide: - 9-11%

Nitrogen: - 50-53%

These above gases are combined called as producer gases.

Some authors have proposed that in order to recovery energy and materials from waste tire efficiently, low-temperature gasification is required [34]. Experiments are carried out in a lab-scale fluidized bed at 400–800^{o}C when equivalence ratio (ER) is 0.2–0.6. Low heat value (LHV) of syngas increases with increasing temperature or decreasing ER, and the yield is in proportion to ER linearly. The yield of carbon black decreases with increasing temperature or ER lightly.

The parameters that are observed from the gasification units are as follows:

(a) Equivalence ratio (ER):

$$\text{ER}=\frac{\text{weight of oxygen (air)/weight dry biomass}}{\text{stoichiometric oxygen (air)/biomass ratio}} \tag{2.17}$$

(b) Euler's number (Eu):

$$Eu=\frac{\Delta P}{\rho u_0^{\,2}} \tag{2.18}$$

(c) Carbon conversion efficiency (η_c) (%):

$$\eta_c=\frac{V_{gs}*1000\left[CH_4\%+CO\%+CO_2\%+2\left(C_2H_4\%+C_2H_6\%+C_2H_2\%\right)*12/28.84\right]}{W\left(1-X_{ash}\right)*C\%}*100 \tag{2.19}$$

The above literature survey indicates that effect of various parameters on reaction kinetics have to be investigated. The computational study for the Euler's number and equivalence ratio has also not been carried out so far. Mathematical expressions for Equivalence ratio and Euler's number for the Fluidized-bed Gasifier involving different system parameters have also to be investigated.

CHAPTER-3

EXPERIMENTATION

Experimentation

Different biomass samples have been studied for gasification in a Fluidized-bed Gasifier. These samples have been analyzed by different analysis techniques for their characteristic study before experimentation in a gasifier.

3.1. RAW MATERIALS USED

3.1.1. Biomass samples:

- Saw dust
- Rice husk
- Rice straw
- Mixed biomass

3.1.2. Bed Materials:

- Silica
- Dolomite
- Calcium carbide
- Aluminum balls

3.2. EXPERIMENTAL PROCEDURE

3.2.1. Cold Model Experimentation:

The experimental set-up is shown in fig-3.1 and 3.2.The unit consists of a reciprocating pump, air blower, U-tube manometer, screw feeder for feeding the biomass and bed materials, bubble cap distributor plate, fluidized bed column and a cyclone separator. At first the starter switch of the air blower was turned on, so that air was flowing to the fluidized bed column through air accumulator and bubble-cap distributor plate. The purpose of using bubble-cap distributor was that these were very resistant to a very high temperature environment. Then screw feeder switch was turned on and the pump connecting to the screw feeder was set at 30-40 rpm speed. A known quantity of the bed materials and the biomass samples were passed to the column at that speed and the feeding rate of the bed material and biomass samples were measured. The velocity at which air was passed to the column, so that complete fluidization took place was noted down and so also the pressure drop across the bed. Similarly the process was repeated for several times. Effects of various system parameters viz. the static bed height, density of the biomass

samples, bed material feeding rate were studied for observing the fluidization characteristics biomass samples which is shown in scope of the experiment (Table-3.1).

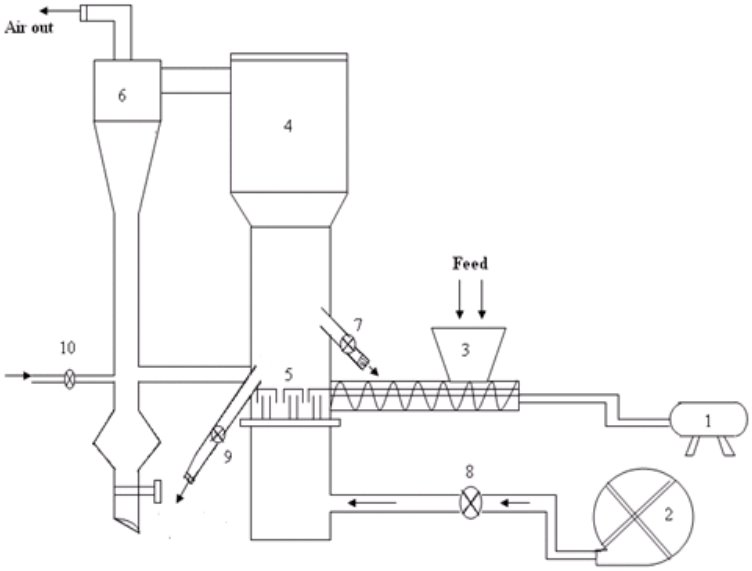

1.	Pump	6.	Cyclone separator
2.	Air blower	7.	Biomass out
3.	Screw feeder	8.	Valve
4.	Fluidized bed reactor	9.	Bed material out
5.	Bubble cap	10.	Valve

Figure-3.1: Experimental set-up of a cold model fluidized bed gasifier

Figure-3.2: Laboratory set-up of a cold model fluidized bed gasifier

Table-3.1: Scope of the experiment

Materials	H_s (cm)	d_p (mm)	ρ_s (kg/m^3)
Silica	2.5	1.65	1602
Silica	3.0	1.65	1602
Silica	4.5	1.65	1602
Dolomite	6.5	1.65	1602
Dolomite	4.5	2.25	1602
Dolomite	4.5	1.65	1602
Calcium carbide	4.5	1.2	1602
Calcium carbide	4.5	0.75	1602
Calcium carbide	4.5	1.65	1602
Al balls	4.5	1.65	2940
Al balls	4.5	1.65	1201
Al balls	4.5	1.65	2700

3.2.2. Hot model experimentation:

The experimental set-up is shown in fig-3.2 and 3.3. The unit consists of an air blower, an air accumulator, U-tube manometer, three reciprocating pumps connecting to three screw feeder for feeding the biomass and bed materials, bubble cap type distributor plate, fluidized bed type gasification unit and a cyclone separator.

At first the starter switch of the air blower is turned on, so that air is passed through the air accumulator to the gasification unit. The gasification unit is made up of mild steel and the insulating material is high alumina. Then the bed material was fed to the gasification unit at a speed of 30-40 rpm. As soon as the bed materials were injected, some external het is given to the bed material by means of liquefied petroleum gas at 20 lpm speed for initial heating purpose. After the bed materials start burning, the supply of LPG gas was stopped. When the bed temperature was reached to 500^{o}C, biomass was fed to the unit at a high speed of about 90 rpm speed to prevent blocking of biomass in the screw feeder section. Then some steam was given to the gasifier section. The pipe through steam passes was made up of copper material, because it has a high thermal conductivity. The gasification process was started and completed by four steps (viz. drying, combustion, gasification and pyrolysis) in the gasifier. The flue gases that were produced along with some dust particle were passed to the cyclone separator to separate the flue gas from the dust particles. The dust particles were collected by gas bags and passed to the

gas sampling and cleaning section for analysis. The air pressure, steam pressure were noted down and so also the bed temperature. The char after combustion were analyzed so that the carbon conversion efficiency was found out.

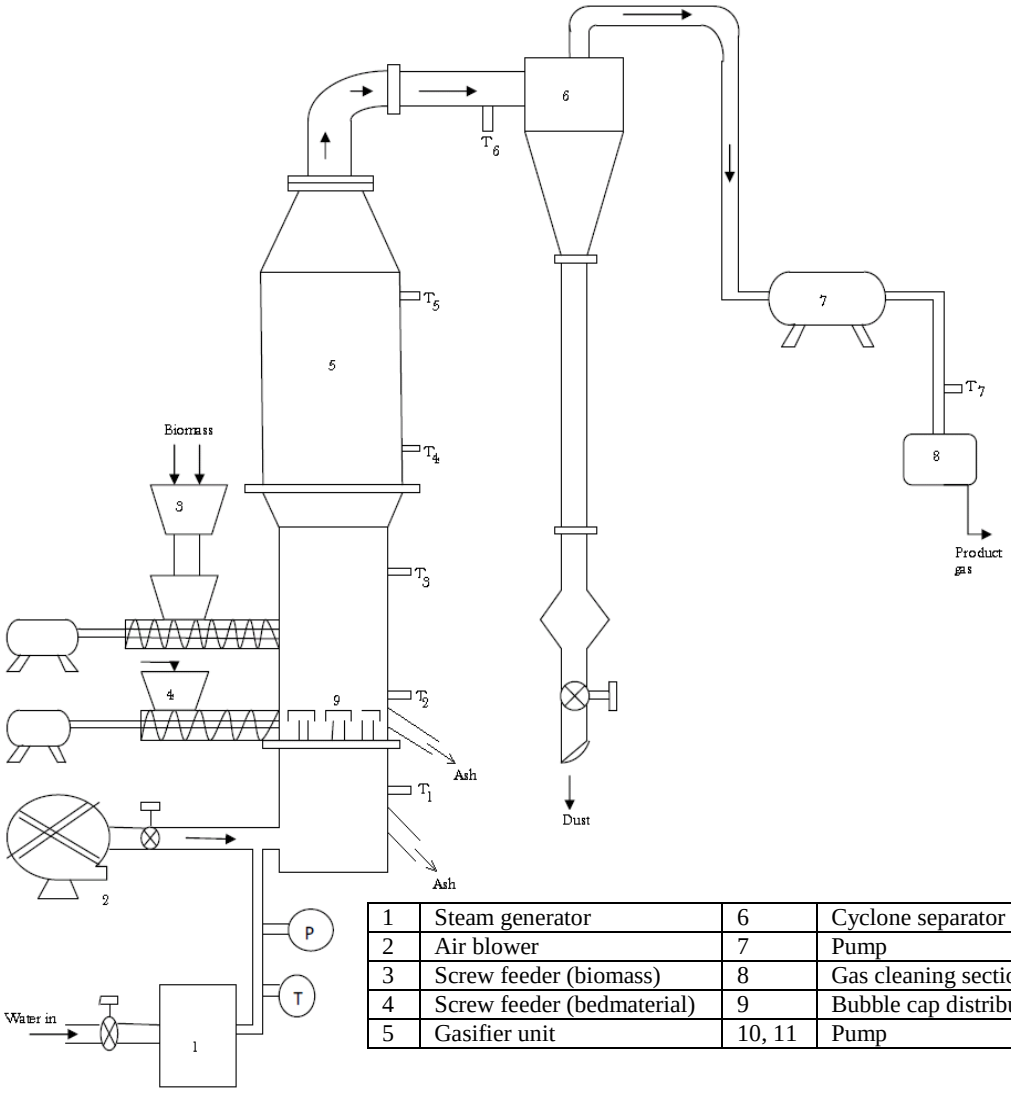

1	Steam generator	6	Cyclone separator
2	Air blower	7	Pump
3	Screw feeder (biomass)	8	Gas cleaning section
4	Screw feeder (bedmaterial)	9	Bubble cap distributor
5	Gasifier unit	10, 11	Pump

Figure-3.3: Experimental set-up of a hot model fluidized bed gasifier

Figure-3.4: Laboratory set-up of a hot model fluidized bed gasifier

CHAPTER-4

PROCESS MODELING

The field of modeling and simulation is as diverse as the concerns of man. Every discipline has developed, or developing, its own models and its own approach and tools for studying these models. The practice of modeling and simulation too is all pervasive. However, it has its own concepts of model description, simplification, validation, simulation and exploration, which are not specific to any particular discipline.

Chemical process modeling is a computer modeling technique used in engineering process. It typically involves using purpose-built software to define a system of interconnected components, which are then solved so that the steady-state or dynamic behavior of the system can be predicted. The system components and connections are represented as a Process Flow diagram.

4.1. COMPUTATIONAL APPROACH USING MAT LAB CODING

The graphical abstract of a fluidized bed reactor is as shown in figure-4.1 for the production of acrylonitril by the ammoxidation of propylene with air in a catalytic fluidized bed reactor. The MATLAB coding has been done by taking the parameters [35] in the mentioned figure which is given as Annexure-1 in the Appendix section. By inserting the values of the above parameters the programme was run and the effects of these parameters on reaction kinetics were observed (Ex. Velocity versus rate constant, height versus conversion, time versus conversion and conversion versus selectivity etc.) and are shown in figures (4.2) to (4.5).

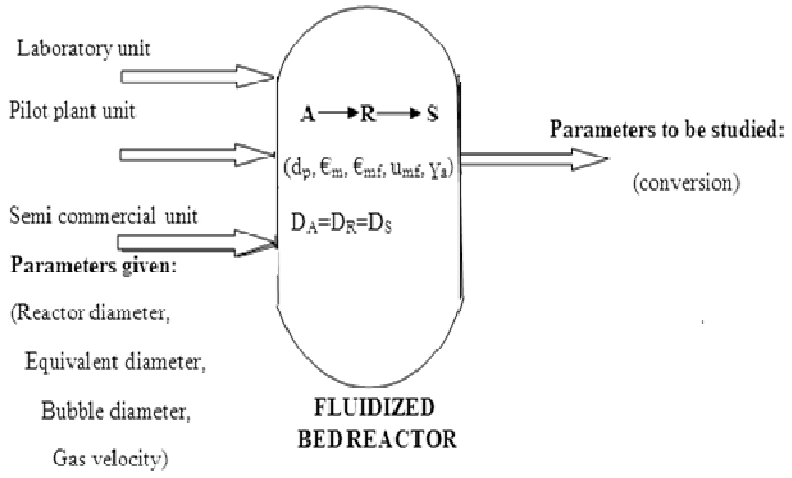

Figure–4.1: Graphical abstract of a fluidized bed reactor

4.2. MODEL EQUATIONS

For all the reactors, on the basis of simple two phase theory, Davidson and Harrison [36] proposed the following bubble rise velocity for only a single bubble:

$$u_{br} = 0.711(gd_p)^{1/2} \tag{4.1}$$

Similarly for velocity of bubbles in bubbling beds of different sizes of solids, Werther [37] had been proposed the following expressions:

(a) For Geldart A solids with $d_t \leq 1m$:

$$u_b = 1.55\{(u_0 - u_{mf}) + 14.1(d_b + 0.005)\}{d_t}^{0.32} + u_{br} \tag{4.2}$$

(b) For Geldart B solids with $d_t \leq 1m$:

$$u_b = 1.6\{(u_0 - u_{mf}) + 1..13{d_b}^{0.5}\}{d_t}^{1.35} + u_{br} \tag{4.3}$$

Then the volume fraction of the bed in the bubbles 'δ' and the average bed voidage 'ε_f' are then related to the voidage of emulsion 'ε_e' by:

$$\varepsilon_f = \delta + (1 - \delta)\varepsilon_e$$

$$\text{Or } 1 - \varepsilon_f = (1 - \delta)(1 - \varepsilon_e) \tag{4.4}$$

In vigorously bubbling beds, where $u_0 \gg u_{mf}$, we may take as an approximation

$$\delta = \frac{u_0}{u_{mf}} \tag{4.5}$$

The distribution of solids in the various regions given by [38]:

$$\gamma_b, \gamma_c, \gamma_e = \frac{\text{volume of solids dispersed in b,c and e respectively}}{\text{volume of bubbles}} \tag{4.6}$$

With δ as the volume fraction of the bed consisting of bubbles, the γ values are related by the expression:

$$\delta(\gamma_b + \gamma_c + \gamma_e) = 1 - \varepsilon_f = (1 - \varepsilon_{mf})(1 - \delta) \tag{4.7}$$

From which

$$\gamma_e = \frac{(1-\varepsilon_{mf})(1-\delta)}{\delta} - \gamma_b - \gamma_c \tag{4.8}$$

With the wake included in the cloud region,

$$\gamma_c = (1 - \varepsilon_{mf})(f_c + f_w) = (1 - \varepsilon_{mf})\left[\frac{3}{u_{br}\varepsilon_{mf}/u_{mf}-1} + f_w\right] \tag{4.9}$$

And γ_b is about 10^{-2} to 10^{-3} by [38].

Cloud volume to bubble volume:

$$f_c = \frac{3}{u_{br}\varepsilon_{mf}/u_{mf}-1} \tag{4.10}$$

Wake volume to bubble volume:

$$f_w\ , \qquad \text{found from Fig. 5.8[41]} \tag{4.11}$$

Fraction of bed in emulsion (*not counting bubble wakes*)

$$f_e = 1 - \delta - f_w\delta \tag{4.12}$$

Harrison [36] derived the following expression for the mass transfer co-efficient between bubble and cloud:

$$K_{bc} = 4.5\left(\frac{u_{mf}}{d_b}\right) + 5.85\left(\frac{\mathcal{D}^{1/2}g^{1/4}}{{d_b}^{5/4}}\right) \tag{4.13}$$

Chiba and Kobayashi [39] solved the fundamental equation governing diffusion through the cloud-emulsion interface as:

$$K_{ce} = 6.77\left(\frac{\mathcal{D}\varepsilon_{mf}(0.711)(gd_b)^{1/2}}{{d_b}^3}\right)^{1/2} \tag{4.14}$$

Now the effective rate constant can be obtained from the given equation:

$$K_{f12} = \left[\gamma_b K_{r12} + \frac{1}{\frac{1}{K_{bc,A}} + \frac{1}{\gamma_c K_{r12} + \frac{1}{\frac{1}{K_{ce,A}} + \frac{1}{\gamma_e K_{r12}}}}}\right]\frac{\delta}{1-\varepsilon_f} \tag{4.15}$$

The concentration of reaction components leaving the bed, denoted by subscript ‘o’ as

$$\frac{C_{Ao}}{C_{Ai}} = exp\left(-K_{f12}\tau\right) \tag{4.16}$$

$$\frac{C_{Ro}}{C_{Ai}} = \frac{K_{f12}}{K_{f34}-K_{f12}}\left[exp\left(-K_{f12}\tau\right) - exp\left(-K_{f34}\tau\right)\right] \tag{4.17}$$

Where

$$K_{fAR} = \frac{K_{r1}}{K_{r12}}K_{f12}$$

Hence the selectivity is given by:

$$S_R = \frac{C_R/C_{Ai}}{X_A} \tag{4.18}$$

The residence time is as follows:

$$\tau = \frac{L_f\left(1-\varepsilon_f\right)}{u_o} \tag{4.19}$$

4.3. RESULTS AND DISCUSSION

4.3.1. Effect of velocity on rate constant:

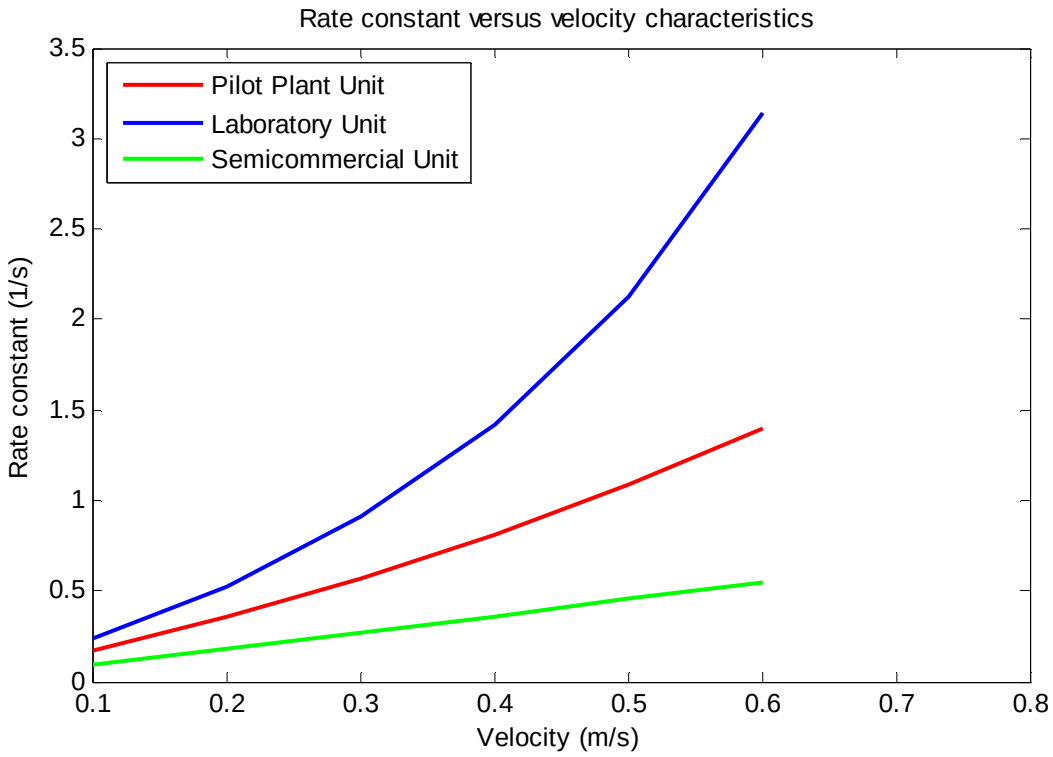

Figure–4.2: Rate constant versus Velocity

Figure-4.2 represents the plot of rate constant versus velocity. From this figure it is observed that as the velocity increases, the rate constant also increases for all the different size of reactors. This is because as the velocity increases, the 'δ'values increases as per eq-(4.5) and then 'ε_f'increases by eq-(4.4) mean while the 'K_{f12}' values increases by eq-(4.15).

Again it is also observed that for the same flow rate the rate constant decreases with increase in reactor size. For Geldart A solids, $u_b \propto d_t^{0.32}$ by eq-(4.2). So by increasing $d_t$value, the $u_b$value increases. Consequently 'δ' value decreases as per eq-(4.5) and 'γ_e' value increases as per eq-(4.8), resulting decrease in 'K_{f12}' as per eq-(4.15).

4.3.2. Effect of bed height on conversion:

Figure-4.3 describes the variation of conversion on bed height for different values of rate constant. And from the plot it is observed that with the increasing value of rate constant the

conversion of the process increases. It is also observed that as the static bed height increases the conversion increases sharply to almost one. The reason behind this may be that the static bed height is directly proportional to the residence time as per eq-(4.19) thus increasing static bed height increases residence time resulting increased conversion as per eq-(4.16).

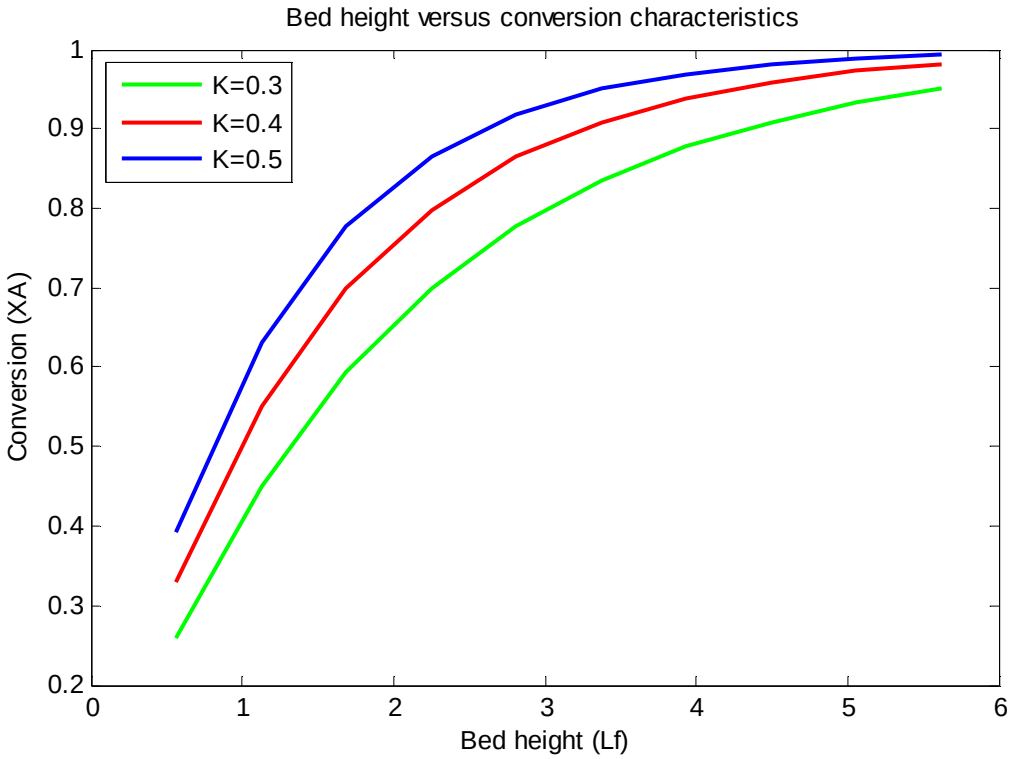

Figure–4.3: Conversion versus Bed height

4.3.3. Effect of time on conversion:

The effect of time on conversion for different values of the rate constant has been shown in figure-4.4. From the figure it is observed that the conversion increases with the increasing values of rate constant. This is due to the fact that the reaction time is directly proportional to the conversion as denoted by eq-(4.16) and eq-(4.17).

4.3.4. Effect of conversion on selectivity:

The relation between the selectivity and the conversion is best described by figure-4.5. From the figure it is observed that the selectivity of the plant decreases with the increase in the conversion for all the values of reaction rate constant because conversion is inversely proportional to the selectivity as per eq-(4.18).

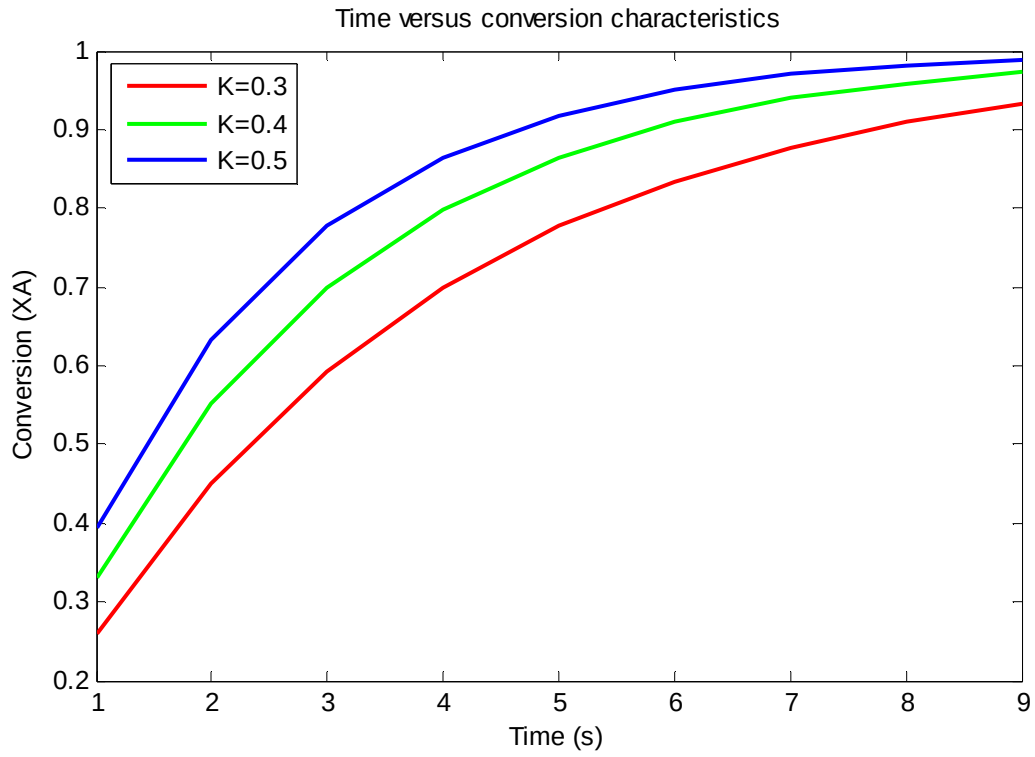

Figure-4.4: Conversion versus Time

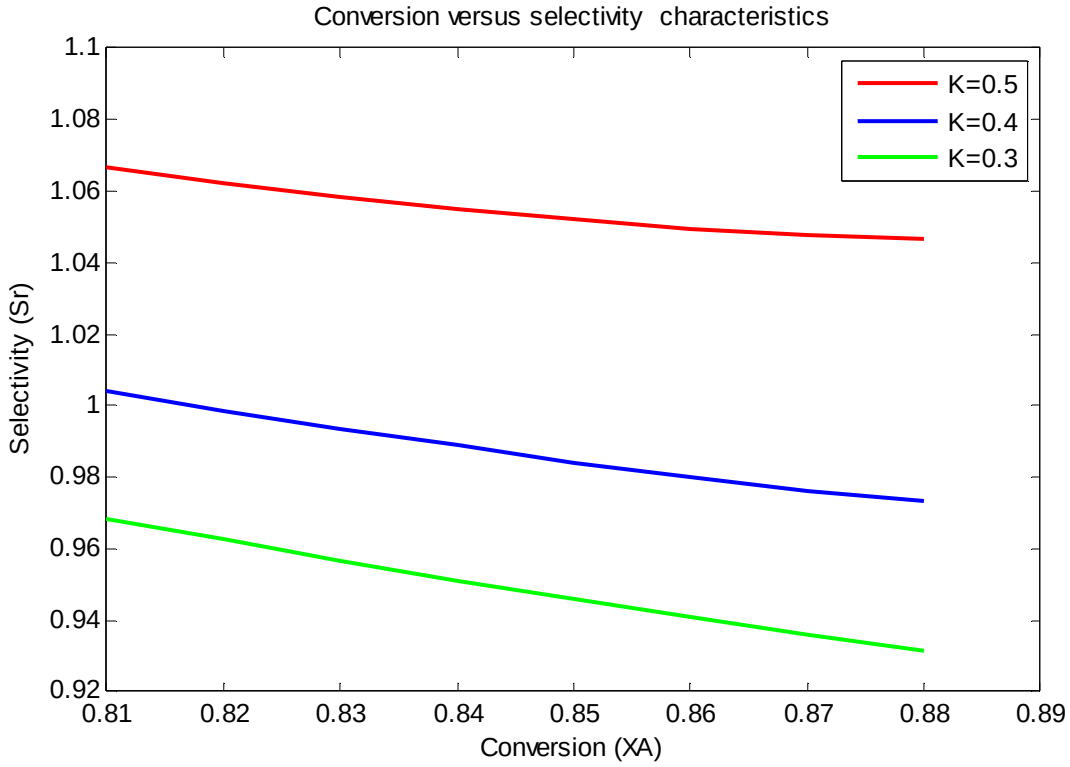

Figure–4.5: Selectivity versus Conversion

CHAPTER-5

OBSERVATION AND RESULTS

Observation and Results

5.1. PRELIMINARY ANALYSIS OF THE BIOMASS SAMPLES

The following analyses have been carried out for the preliminary analysis of the different biomass samples. These are as follows.

- ❖ Ultimate analysis
- ❖ Thermo gravimetric Analysis (TGA)
- ❖ Proximate analysis
- ❖ Analysis other properties

5.1.1. Ultimate analysis:

Determination of total carbon, hydrogen, nitrogen, oxygen and sulphur percentages in the biomass sample comprises its ultimate analysis [40]. With the ultimate analysis of all these biomass samples, the following results were obtained as shown in Table-5.1.

Table-5.1: Results of Ultimate Analysis

Types of biomass	Amount(mg)	Carbon(%)	Hydrogen(%)	Nitrogen(%)	Sulphur(%)	Oxygen(%)
Saw dust	8.94	45.78	5.32	0	0.07	48.83
Rice husk	9.52	38.45	4.96	0.82	0.18	55.59
Rice straw	5.74	36.60	4.55	0.46	0.21	58.17
Mixed biomass	7.73	40.85	5.04	0.57	0.12	53.42

5.1.2. TGA:

The TGA (Thermo gravimetric Analysis) of these biomass samples was carried out and the result is shown in Fig.-5.1

5.1.3. Proximate analysis:

Determination of moisture content, volatile matter, ash content and fixed carbon in the biomass sample comprises the proximate analysis. The proximate analysis for different biomass samples give the following results which are listed in Table-5.2.

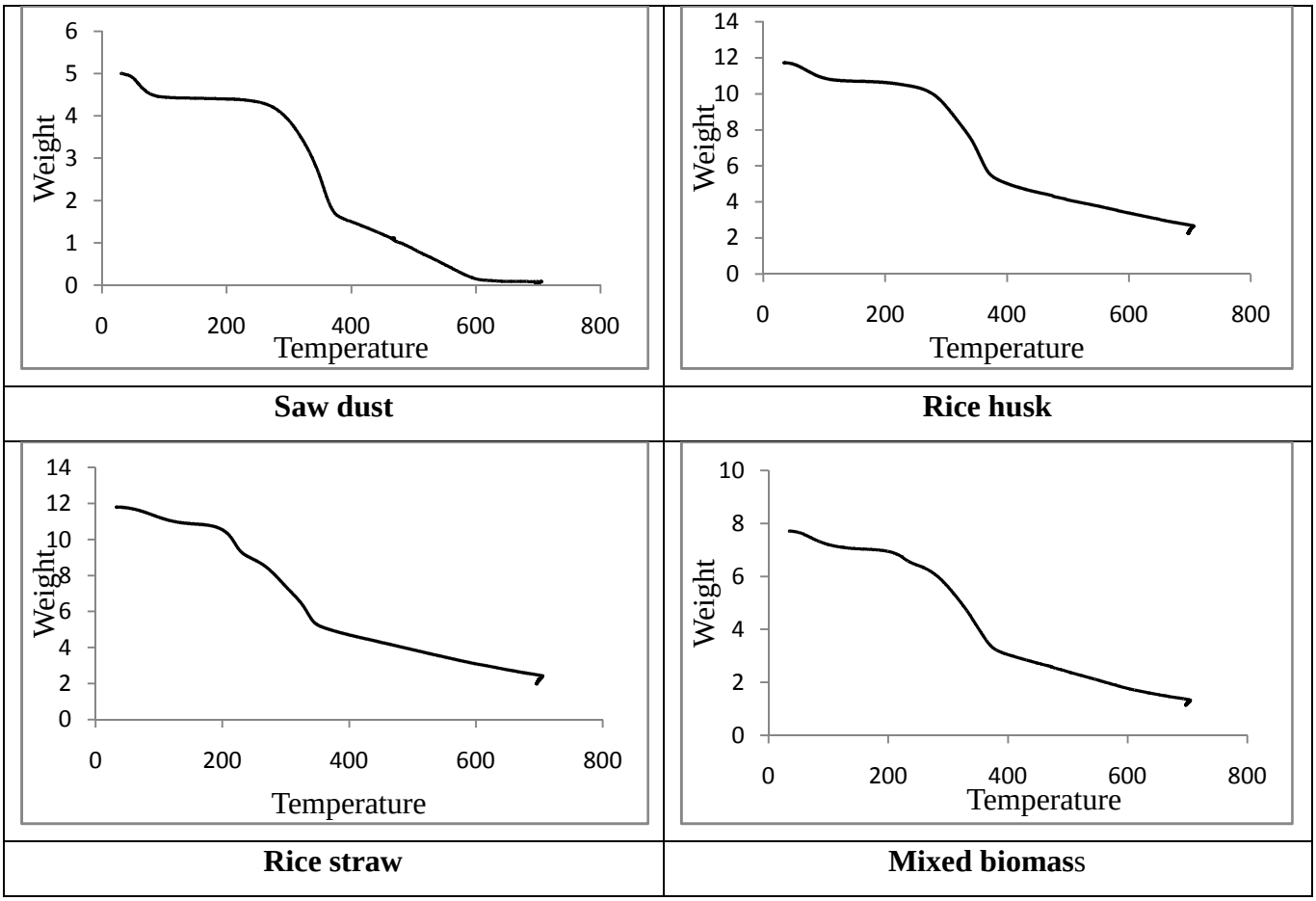

Figure-5.1: Results of TGA for different biomass samples

Table-5.2: Results of Proximate Analysis for different biomass samples

Biomass samples	Moisture content (%)	Volatile matter (%)	Ash content (%)	Fixed carbon (%)
Saw dust	8.8	87.57	1.94	1.69
Rice husk	12.34	64.37	2.83	20.46
Rice straw	9.38	69.53	3.04	18.05
Mixed biomass	11.77	70.49	1.14	16.66

5.1.4. Analysis of other properties:

There are some another properties like bulk density, mean particle diameter, sphericity and porosity were measured for the biomass samples, which are as shown in Table-5.3.

(a) Bulk density:

The bulk density of the biomass samples are otherwise known as tapped density. It is calculated by putting the samples in a container whose volume can be measured. By tapping the materials were tightly packed in the container. After that the mass of the sample was weighted in an electronic balance and by dividing the mass of the sample to the volume, the bulk density can be found out.

Sample calculation: (saw dust)

Weight of the saw dust= 3.370 gm

Volume= $3.14*(2.6)^2*(2.6)/ 4= 13.8\ cm^3$

Density (ρ) = 3.370/13.8 = 0.2442 gm/cm^3= 244.2 kg/m^3

(b) Mean particle diameter:

The mean particle size is found out by sieve analysis.

Sample calculation: (saw dust)

Size= average of mesh openings for sieves of BSS-12 and 72 (-12+72)

= (1.4+0.212)/2 = 0.81 mm

(c) Porosity or void fraction:

Porosity or void fraction can be defined as the amount of empty space in the bed. It can be found out by subtracting the volume of solid from the bed volume.

Sample calculation: (saw dust)

Weight of saw dust= 3.58 gm

Volume of saw dust= weight/density = 3.58/244.2= $1.47*10^{-5}\ m^3$

Volume of the bed= $3.14*(2.6)^2*4.8= 25.47\ cm^3=25.47*10^{-6}\ m^3$

Solid fraction= $1.47*10^{-5}/25.47*10^{-6}$ = 0.58

Void fraction= 1-0.58 = 0.42

(d) Sphericity:

The shape of an individual particle is conveniently expressed in terms of the sphericity, which is independent of particle size. For a non spherical particle, the sphericity is given by the following expression [41]:

$$\phi_s = \frac{6 v_p}{D_p s_p} \quad (5.1)$$

Some authors calculated the sphericity of particle by the following formula [42]:

$$\frac{1-\varepsilon}{\phi_s} = 0.231 \log(D_p) + 1.417 \quad (5.2)$$

Table-5.3: Data on other properties for different biomass samples

Biomass samples	Bulk density (kg/m^3)	Mean particle diameter (mm)	Sphericity	Porosity
Saw dust	244	0.81	0.7	0.42
Rice husk	426	0.53	0.81	0.37
Rice straw	153	2.9	0.46	0.56
Mixed biomass	232	1.7	0.75	0.33

5.2. IMPORTANCE OF CHEMICAL FORMULA

The calculation of chemical formula is important to determine the stoichiometric amount of air required for the combustion of the biomass samples.

Sample calculations for saw dust:

(A) Amount of carbon= (45.78*8.94)/100= 4.09

Amount of hydrogen= (5.32*8.94)/100= 0.48

Amount of nitrogen= 0

Amount of sulphur= (0.07*8.94)/100= 0.0063

Amount of oxygen= (48.83*8.94)/100= 4.37

(B) No. of moles of carbon= 4.09/12= 0.34

No. of moles of hydrogen= 0.48/1= 0.48

No. of moles of nitrogen= 0

No. of moles of sulphur= 0.0063/32= 0.00019

No. of moles of oxygen= 4.37/16= 0.27

Hence the total no. of moles= 0.34+0.48+0.00019+0.27=1.09019

(C) We know

No of moles= mass/molecular weight

so, molecular weight = mass/ no of moles= 8.94/1.09019= 8.2

(D) Amount of carbon= (8.2*45.78)/ 100= 3.75

Atoms of carbon= 3.75/12= 0.31

Amount of hydrogen= (8.2*5.32)/100= 0.44

Atoms of hydrogen= 0.44/1= 0.44

Amount of nitrogen= 0

Atoms of nitrogen= 0

Amount of sulphur=(8.2*0.07)/100=0.0057

Atoms of sulphur= 0.0057/32=0.00018=0

Amount of oxygen= (48.83*8.2)/100= 4

Atoms of oxygen= 4/16= 0.25

Hence the chemical formula is $CH_{1.4}O_{0.8}$

In the above similar way the chemical formulas of all the biomass samples were calculated, which are given in Table-5.4.

Table-5.4: Chemical formulas of biomass samples

Biomass samples	Chemical formula
Saw dust	$CH_{1.4}O_{0.8}$
Rice husk	$CH_{1.6}O_{1.1}$
Rice straw	$CH_{1.5}O_{1.2}$
Mixed biomass	$CH_{1.5}O$

5.3. EXPERIMENTAL RESULTS FOR COLD MODEL UNIT

Correlations have been developed for finding out the values of equivalence ratio (ER) and Euler's number (Eu) by varying different system parameters, which are as follows:

$$ER = 1.039\left[\left(\frac{H_s}{D_c}\right)^{0.205}\left(\frac{d_p}{D_c}\right)^{0.233}\left(\frac{\rho_s}{\rho_f}\right)^{0.09}\right] \quad (5.3)$$

$$Eu = 4E+06\left[\left(\frac{H_s}{D_c}\right)^{0.016}\left(\frac{d_p}{D_c}\right)^{0.046}\left(\frac{\rho_s}{\rho_f}\right)^{-0.099}\right] \quad (5.4)$$

The correlation plots for equivalence ratio (ER) and Euler's number (Eu) are shown in Fig-5.2 and 5.3 respectively. The observed data for the same with the different parameters have been shown in Table-5.5 and 5.6 respectively.

Table-5.5: Comparison between calculated values of ER obtained from dimensionless analysis with the experimentally observed values.

H_s/D_c	d_p/D_c	ρ_s/ρ_f	Product	ER-Exp	ER-Cal	% Dev
0.167	0.011	1501.4	0.49	0.49	0.486	-0.721
0.2	0.011	1501.4	0.51	0.5	0.505	0.971
0.3	0.011	1501.4	0.55	0.53	0.549	3.546
0.43	0.011	1501.4	0.59	0.59	0.591	0.170
0.3	0.015	1501.4	0.59	0.58	0.589	1.699
0.3	0.011	1501.4	0.55	0.55	0.548	-0.218
0.3	0.008	1501.4	0.51	0.5	0.509	1.922
0.3	0.005	1501.4	0.45	0.46	0.456	-0.689
0.3	0.011	1125.6	0.54	0.54	0.534	-0.973
0.3	0.011	1501.4	0.55	0.57	0.548	-3.719
0.3	0.011	2530.5	0.57	0.58	0.575	-0.825
0.3	0.011	2755.4	0.58	0.59	0.579	-1.756

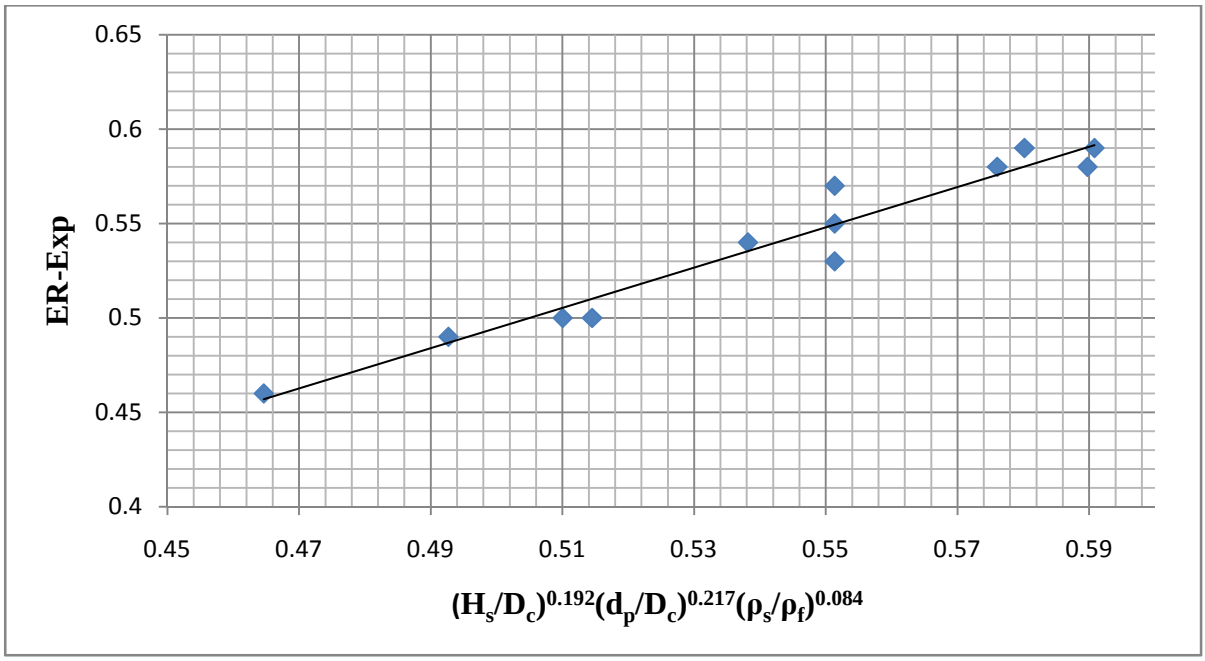

Figure-5.2. Correlation plot for ER against the system parameters

Table-5.6: Comparison between calculated values of Eu obtained from dimensionless analysis with the experimentally observed values.

Hs/Dc	dp/Dc	ρs/ρf	Product	Eu-exp	Eu-cal	% Dev
0.167	0.011	1501.4	0.312	1337529	1524969.6	14.01
0.2	0.011	1501.4	0.313	1363386	1529524.7	12.19
0.3	0.011	1501.4	0.315	1366528	1539816.7	12.68
0.43	0.011	1501.4	0.318	1369164	1549012.9	13.14
0.3	0.015	1501.4	0.321	1335665	1562094.2	16.95
0.3	0.011	1501.4	0.315	1366528	1539816.8	12.68
0.3	0.008	1501.4	0.310	1332678	1517273.9	13.85
0.3	0.005	1501.4	0.302	1263782	1484604.5	17.47
0.3	0.011	1125.6	0.326	1478464	1584474.3	7.17
0.3	0.011	1501.4	0.315	1440357	1539816.8	6.91
0.3	0.011	2530.5	0.296	1335665	1462077.4	9.46
0.3	0.011	2755.4	0.293	1325353	1449775.1	9.39

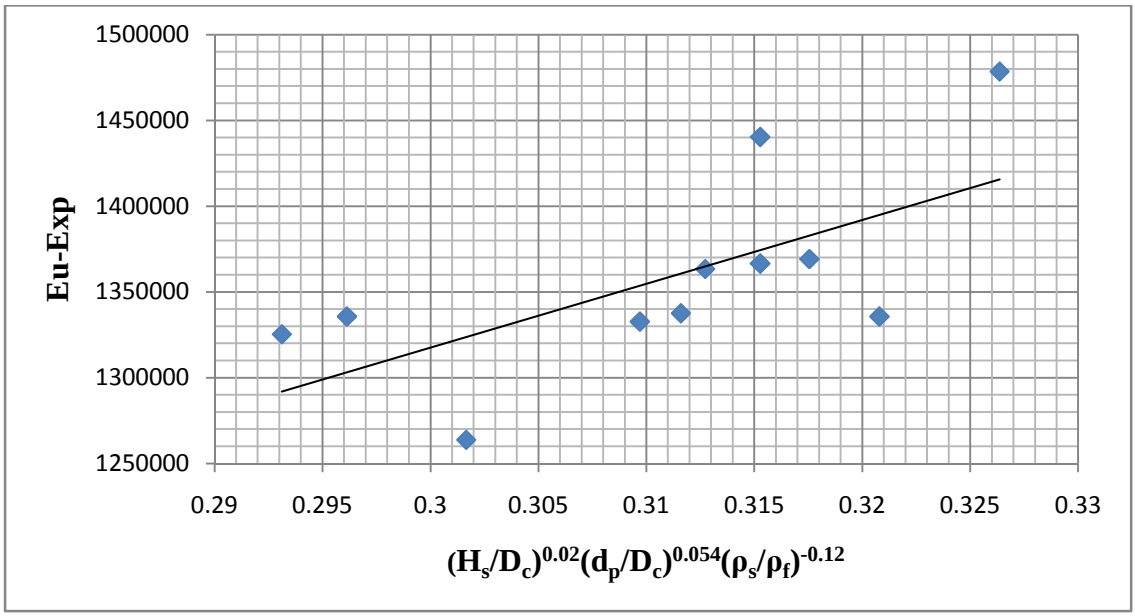

Figure-5.3. Correlation plot for Eu against the system parameters

Calculated values of ER and Euler's number have been compared with the experimentally observed vales for the same. The comparison plots are shown in Fig-5.4(a) and 5.4(b) respectively.

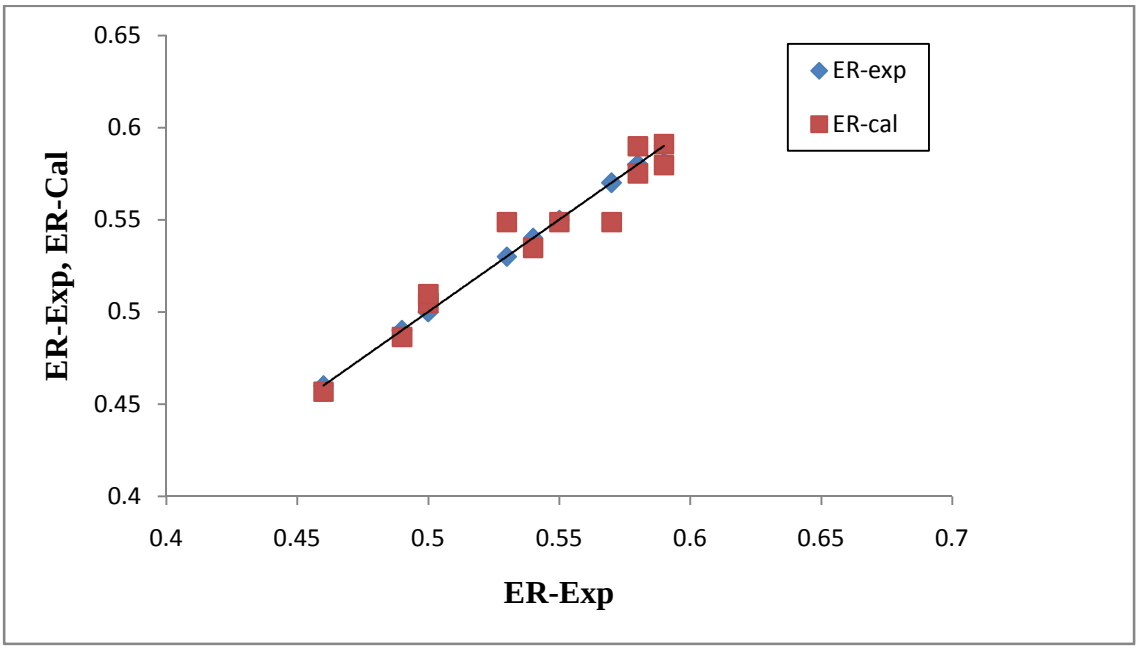

Figure- 5.4 (a) Comparison of calculated values of equivalence ratio obtained from Dimensionless analysis against the experimental ones

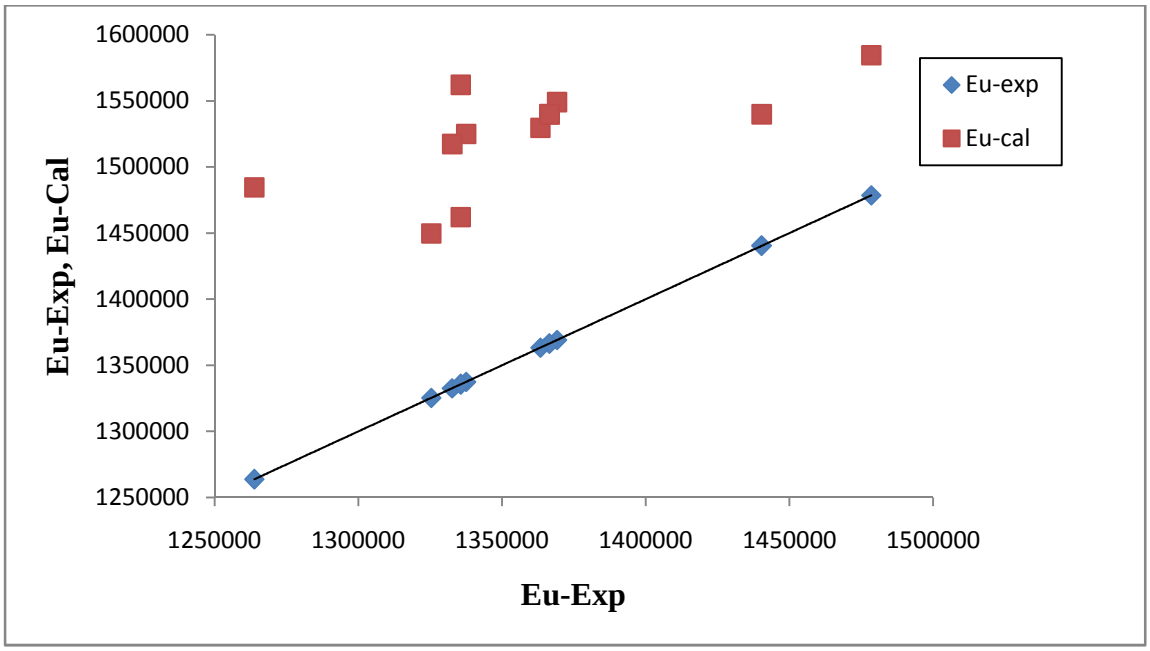

Figure-5.4. (b) Comparison of calculated values of Euler's number obtained from Dimensionless analysis against the experimental ones

5.4. EXPERIMENTAL RESULTS FOR HOT MODEL UNIT

The hot model experiment was carried out for the calculation of the carbon conversion efficiency at the condition as given below.

Biomass	Bed material	Bed temperature (^oC)	Bed height(cm)	Pressure drop (N/m^2)	Air velocity (m/s)	Air flow rate (m^3/s)
Saw dust	Silica	600	2.5	3712	0.051	0.00092

The reactions taking place in hot model are:

1. Oxidation reaction:

$$C + O_2 = CO_2$$

$$H_2 + ½\ O_2 = H_2O$$

2. Reduction reaction:

$$CO_2 + C = 2CO$$

$$C + H_2O = CO + H_2$$

$CO_2 + H_2 = CO + H_2O$

$C + 2H_2 = CH_4$

From the Ultimate analysis of the biomass samples and by using the stoichiometric calculations the following product gas compositions were obtained.

Table-5.7: Product gas composition from the hot model experiment

Components	Mass (kg)	Mass% (wet basis)
CH_4	0.54	1.4
CO	3.73	9.8
H_2O	2.4	6.3
CO_2	0.18	0.47
O_2	1.68	4.4
H_2	3.87	10.2
N_2	25.5	67

Hence the carbon conversion efficiency (η_c) was found to be:

$$\eta_c = [((37.9(1.4 + 9.8 + 0.47)12/28.84)/(5(1 - 0.017)45.8))] * 100 = 81.7\%$$

CHAPTER-6

DISCUSSION AND CONCLUSION

Discussion and Conclusion

6.1. COLD MODEL

The experiments have been conducted in a cold-model unit of the experimental set up i.e. of the laboratory scale gasification unit using the equations (2.17) and (2.18). Several experiments were carried out by varying the different system parameters like density, static bed heights and bed particle diameter etc. It is observed from the figure-(6.1) and (6.5) that with increase in static bed height, the equivalence ratio and the Euler's number both increases gradually with a certain trend and also with the bed particle size where as in the case of varying density of the bed materials, the equivalence ratio increases but the Euler's number decreases. The effects of individual parameters on ER and Eu has also been observed by the MAT LAB coding (from figure (6.2) to (6.4) and figure (6.6) to (6.8) respectively) and it also shows the similar trends as discussed above. The calculated values of ER and Eu obtained from the developed correlation were compared with the values those values obtained from the programming. From the comparison, the percentage deviation is less in both the cases (i.e. the equivalence ratio and the Euler's number) which is shown in Table-6.1.

The overall changes in values of equivalence ratio and Euler's number were observed from the developed correlations (Eq. No. 5.3 and 5.4). It is observed that with the increase in static bed height and particle size both the Equivalence ratio and Euler's number increase, but in varying particle density, the ER values increase and the Eu values decrease. Experimental values of equivalence ratio and Euler's number are obtained by Eq. no.-(2.17) and (2.18). Calculated values of these values obtained through Eq. no.-(5.3) and (5.4) are compared against the experimental values. The comparison plots for ER and Eu by different methods are shown in Figure-5.4 which shows a good agreement. The standard deviation, mean deviation and correlation fit in terms of Chi-square (ξ^2) (Table-6.2) imply that the developed correlations for the ER and Eu are satisfactory.

6.1.1. Effects of individual system parameters on ER:

6.1.1 (A). Effects of individual system parameters on ER by dimensionless analysis:

Hs/Dc	ER
0.167	0.49
0.2	0.5
0.3	0.53
0.43	0.59

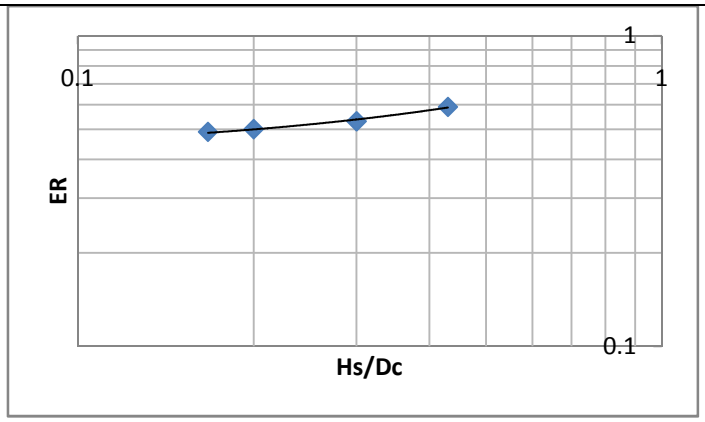

Dp/Dc	ER
0.015	0.58
0.011	0.55
0.008	0.5
0.005	0.46

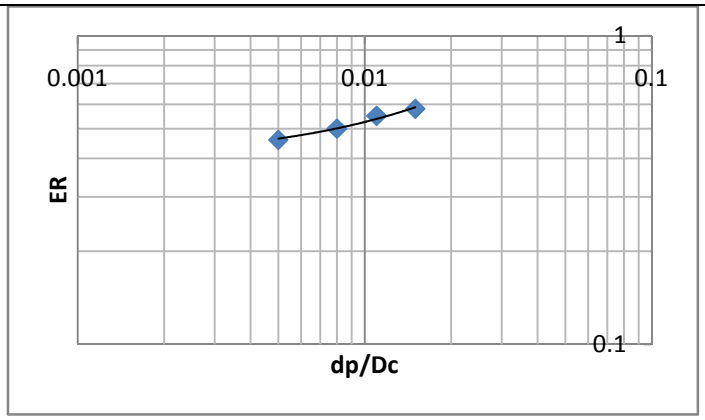

ρs/ρf	ER
1125.6	0.54
1501.4	0.57
2530.5	0.58
2755.4	0.59

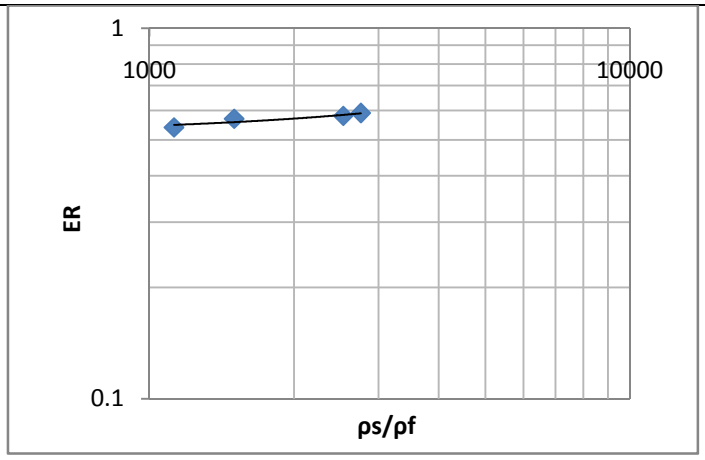

Figure-6.1. Effect of individual system parameters on ER

6.1.1 (B). Effects of individual system parameters on ER by using MAT LAB:

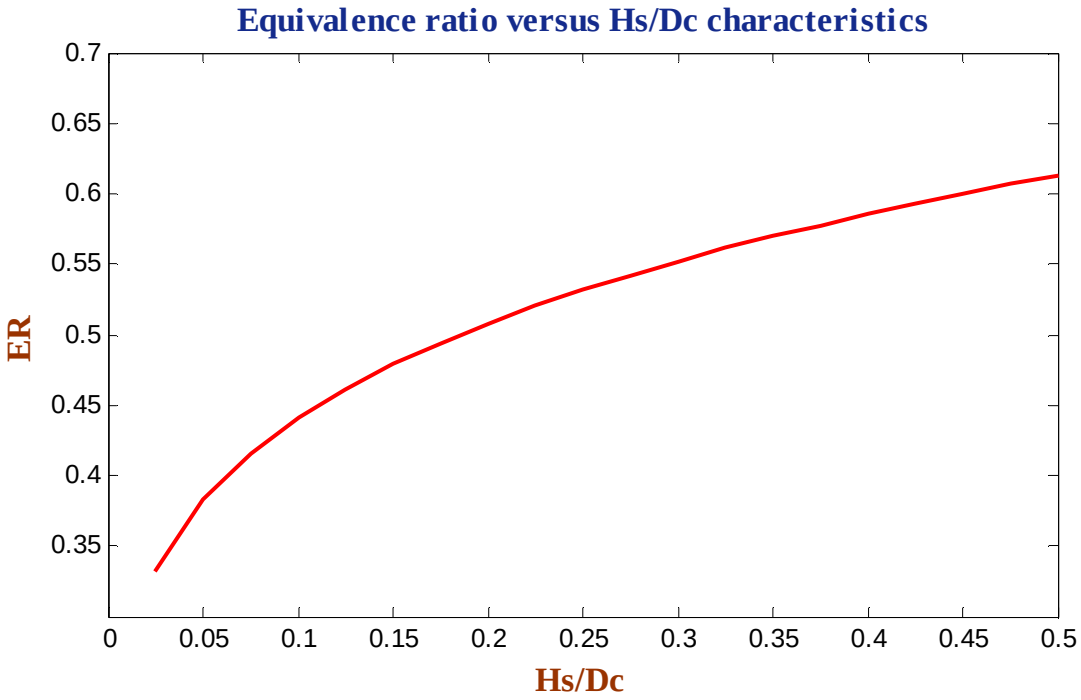

Figure-6.2. Effects of static bed height on Equivalence ratio

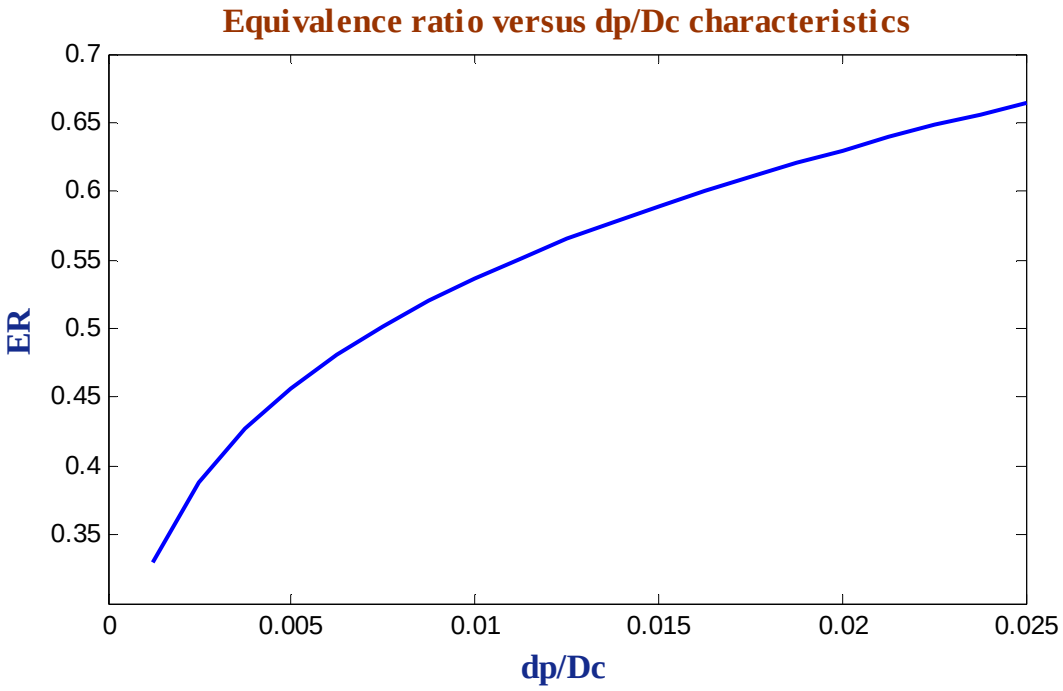

Figure-6.3. Effects of particle diameter on Equivalence ratio

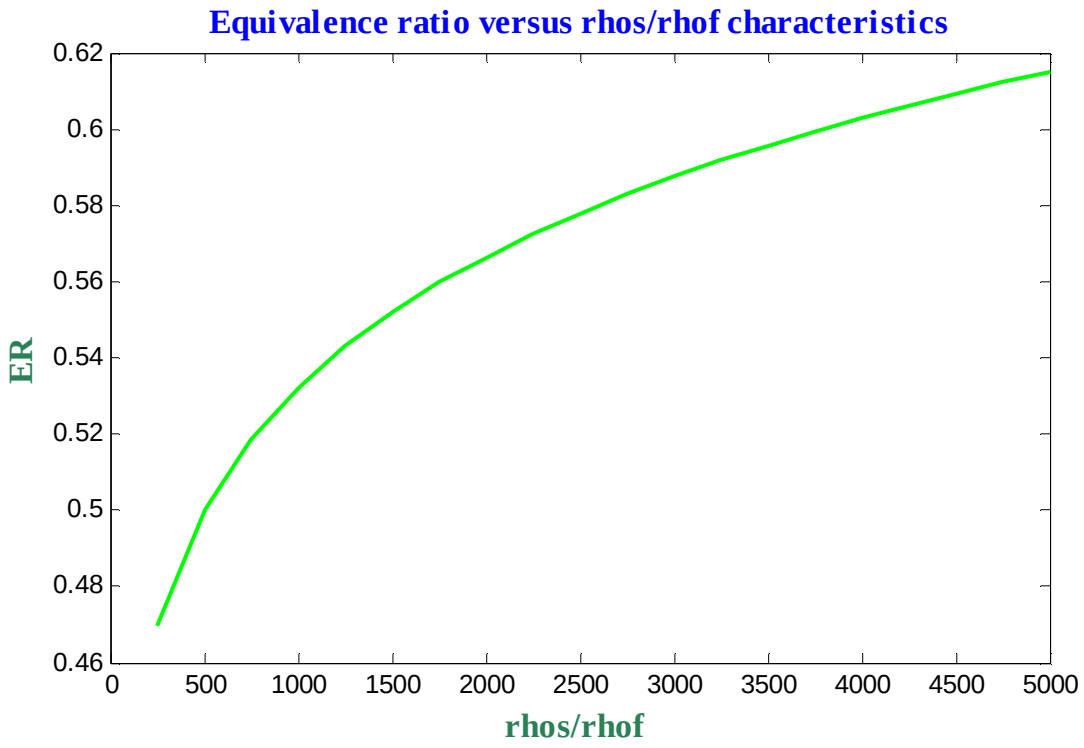

Figure-6.4. Effects of particle density on Equivalence ratio

6.1.2. Effects of individual system parameters on Eu:

6.1.2 (A). Effects of individual system parameters on Eu by dimensionless analysis:

Hs/Dc	Eu
0.167	1337529
0.2	1363386
0.3	1366528
0.43	1369164

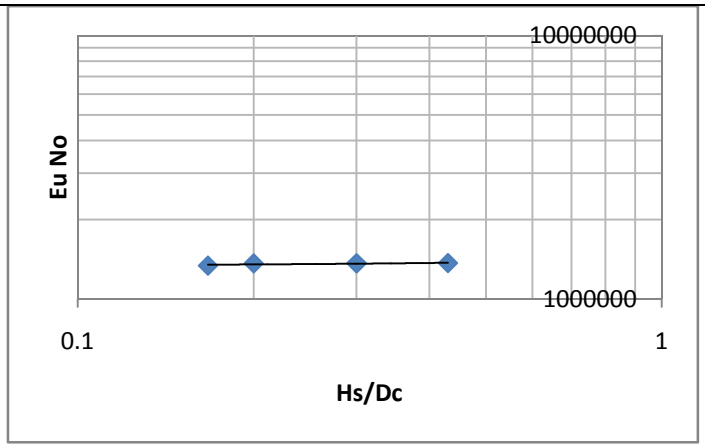

Dp/Dc	Eu
0.015	1335665
0.011	1366528
0.008	1332678
0.005	1263782

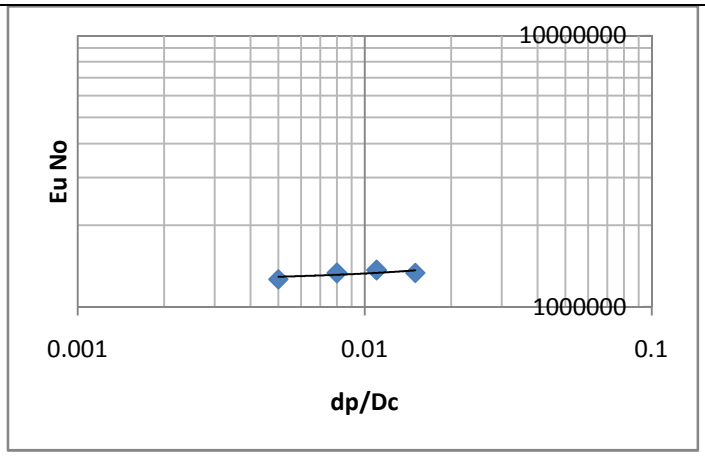

ρs/ρf	Eu
1125.6	1478464
1501.4	1440357
2530.5	1335665
2755.4	1325353

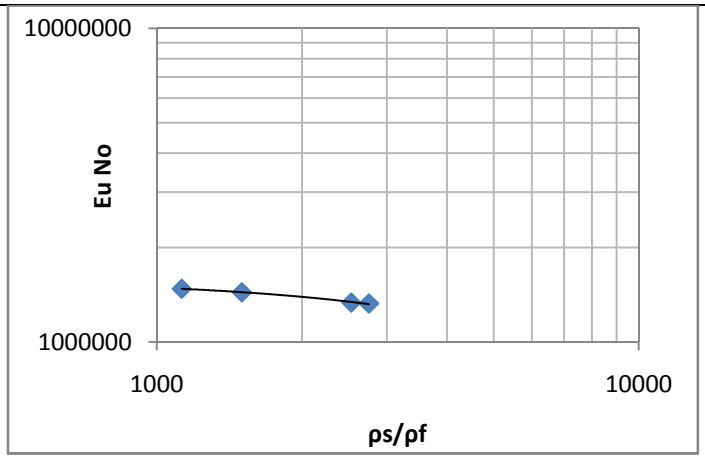

Figure-6.5. Effect of individual system parameters on Eu

6.1.2 (B). Effects of individual system parameters on Eu by using MAT LAB:

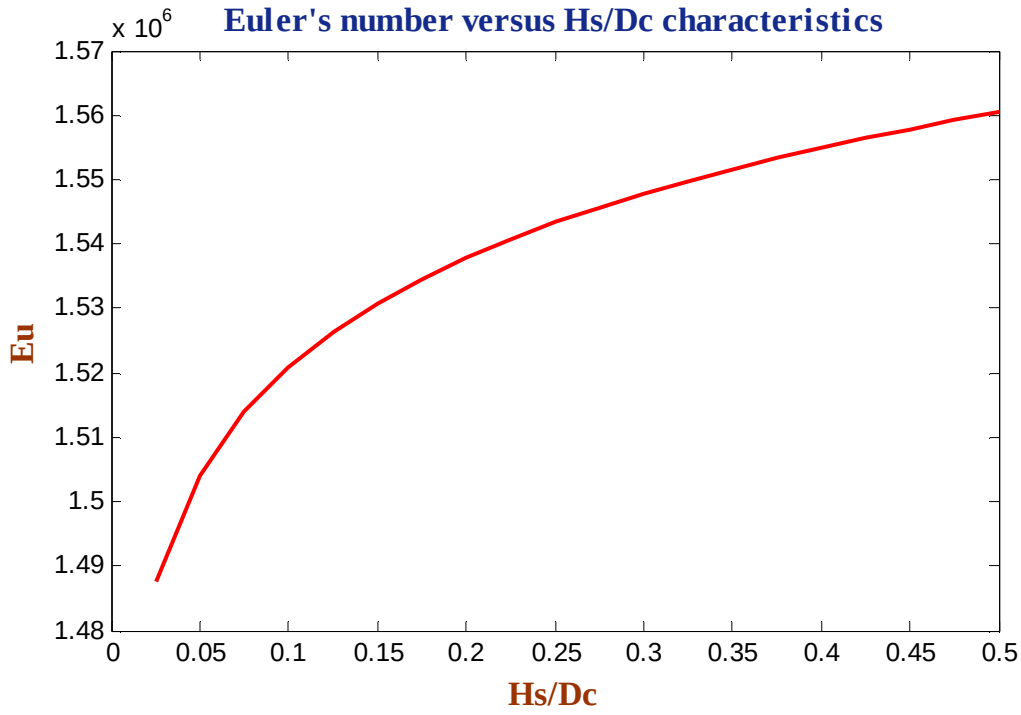

Figure-6.6. Effects of static bed height on Euler's number

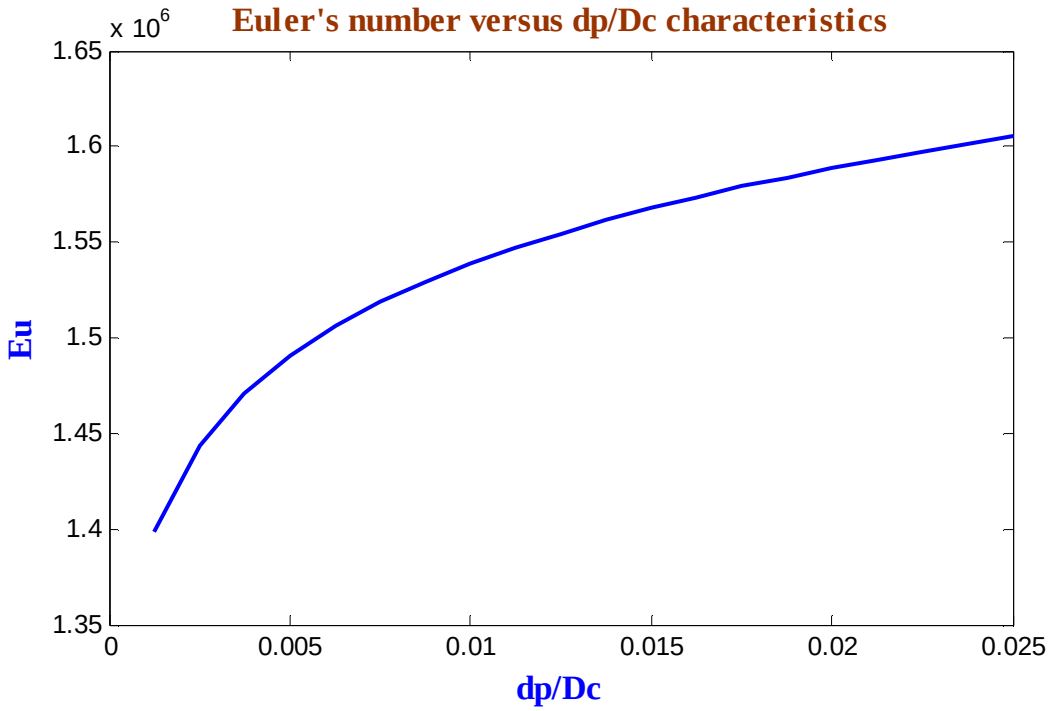

Figure-6.7. Effects of particle diameter on Euler's number

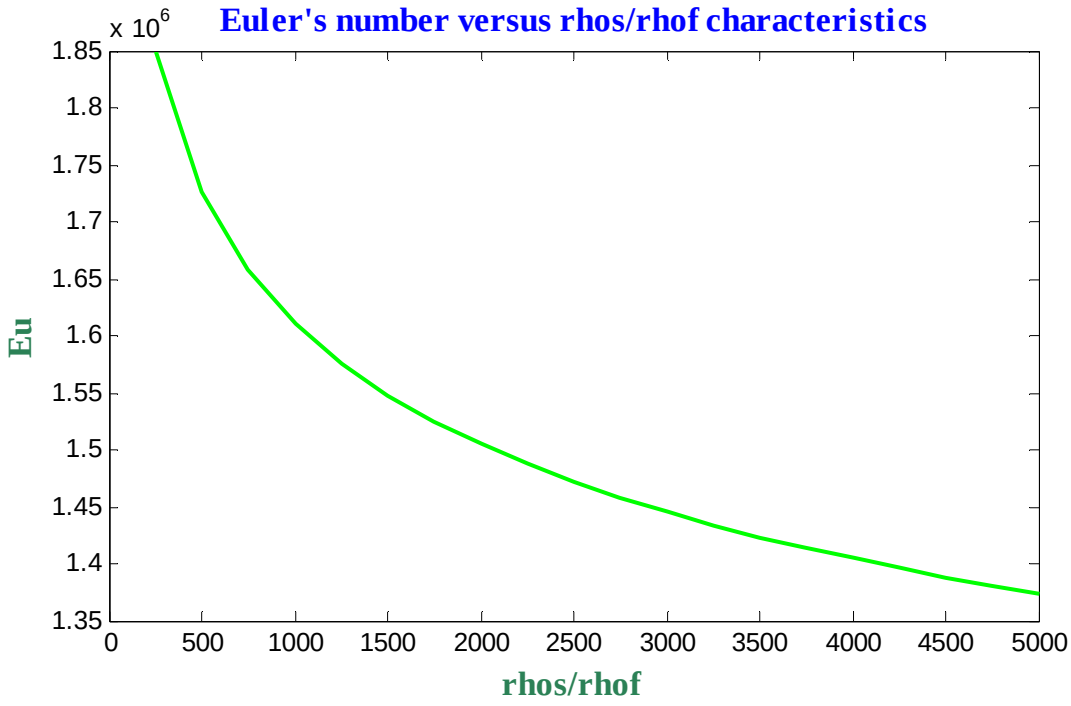

Figure-6.8. Effects of particle density on Euler's number

Table-6.1: Comparison of calculated values of the ER and Eu using MAT LAB and the experimental values.

(A) For static bed height

Parameters	**Equivalence ratio (ER)**			**Euler's number (Eu)**		
H_s/D_c	ER-exp	ER-prog	% dev	Eu-exp	Eu-prog	% dev
0.167	0.49	0.487	-0.61	1337529	1532800	14.6
0.2	0.5	0.508	1.6	1363386	1537800	12.8
0.3	0.53	0.552	4.15	1366528	1547800	13.3
0.43	0.59	0.59	0	1369164	1556500	13.7

(B) For particle diameter

Parameters	**Equivalence ratio (ER)**			**Euler's number (Eu)**		
d_p/D_c	ER-exp	ER-prog	% dev	Eu-exp	Eu-prog	% dev
0.015	0.58	0.589	1.55	1335665	1567900	17.4
0.011	0.55	0.55	0	1366528	1547300	13.3
0.008	0.5	0.51	2	1332678	1526500	14.5
0.005	0.46	0.456	-0.86	1263782	1490600	17.9

(C) For particle density

Parameters	**Equivalence ratio (ER)**			**Euler's number (Eu)**		
ρ_s/ρ_f	ER-exp	ER-prog	% dev	Eu-exp	Eu-prog	% dev
1125.6	0.54	0.535	-0.92	1478464	1558500	5.41
1501.4	0.57	0.552	-3.16	1440357	1543800	7.18
2530.5	0.58	0.578	-0.34	1335665	1483900	11.09
2755.4	0.59	0.583	-1.18	1325353	1467500	10.72

Table-6.2: Percentage deviations of the calculated values of the ER and Eu from the experimentally observed values and chi square values for the correlation-fit.

Equivalence Ratio(ER)			Euler's number(Eu)		
Standard deviation, %	Mean Deviation,%	Chi square(ξ^2)	Standard deviation, %	Mean deviation%	Chi square(ξ^2)
1.89	-0.049	0.0002	2.64	10.8	18685.04

6.2. HOT MODEL

Parametric tests have been performed by varying the temperature, equivalence ratio and biomass particle sizes, to determine their effects on carbon conversion efficiency. The carbon conversion efficiency was found to be 81.7% at the bed temperature of 600^{o}C, which shows that almost complete combustion takes place in the fluidized bed gasifier.

6.3. CONCLUSION

The MATLAB coding was developed for the catalytic fluidized bed reactor system to study the effect of various important hydrodynamic, operating and design parameters on the reaction rate kinetics. With the help of the above coding the simulation was done in a FBR and from that we conclude that the effective rate constant of the process increases with the increasing inlet gas flow rate decreases with the increase in reactor size. The percentage of conversion during the process shows an increase in trend with the static bed height, residence time and the rate constant but the selectivity of the process decreases with increasing conversion and reaction rate constant. The calculated values of the Equivalence ratio and the Euler's number obtained through dimensionless analysis and MATLAB programming have been compared with the experimentally observed values for the laboratory scale cold-model fluidized bed gasifier unit. The comparison shows that the percentage deviation between the calculated values and the values obtained through MAT LAB programming are very less. The standard deviations for the Equivalence ratio and the Euler's number were found to be 1.89 and 10.8 respectively which validates the developed correlations. The chi-square test justifies the correlation fit to be satisfactory. This indicates that these correlations can be used suitably over a wide range of

system parameters. These models can be suitably scaled up for pilot plant units or for industrial uses. The developed correlations can also be used as the basis of designs for the industrial fluidized bed gasifier. The carbon conversion efficiency for the hot-model experimental set-up was found to be 81.7%.

6.4. SCOPE OF THE WORK

In the present work, experiments were carried out in cold model unit only and one trial run can possible in the hot model unit. The carbon conversion efficiency and equivalence ratios were found out for the hot model unit of the fluidized bed gasifier. Therefore other calculations (viz. calorific values of the biomass samples and steam decomposition) can also be carried out for the hot model unit. Various modeling techniques like CFD approaches can also be applied on the biomass gasification process. Now-a-days the ASPEN PLUS software also finds wide scope to simulate the biomass gasification process.

Nomenclature

K_p	:	Chemical rate constant, kg/(cm^2 s atm o_2)
R	:	Universal gas constant, kJ $mol^{-1}K$
T_p	:	Absolute temperature, K
δH°	:	Change in standard enthalpy,kJ mol^{-1}
δS°	:	Change in standard entropy,J mol^{-1} K^{-1}
δG°	:	Change in standard free energy,kJ mol^{-1}
b	:	Langmuir constant, l mol^{-1}
b_1	:	Langmuir constant at 25^oc
b_2	:	Langmuir constant at 45^oc
T	:	Temperature, degree centigrade
T_1	:	Temperature at 25^oc
T_2	:	Temperature at 45^oc
V_{gs}	:	Dry product gas flow rate, Nm^3/h
W	:	Dry biomass feeding rate, g/h
X_{ash}	:	Ash content in the feed
C%	:	Carbon content in the ultimate analysis of biomass.
u_{br}	:	Bubble rise velocity, m/s
u_{mf}	:	Minimum fluidization velocity, m/s
u_b	:	Velocity of bubbles in bubbling bed, m/s
u_o	:	Superficial velocity, m/s
g	:	Gravitational constant, m/s^2
d_p	:	Diameter of particle, µm
d_t	:	Reactor diameter, m
d_b	:	Bubble diameter, m
f_c	:	Cloud volume to bubble volume
f_w	:	Wake volume to bubble volume
f_e	:	Fraction of bed in emulsion
D	:	Diffusivity, m^2/s
K_{bc}	:	Inter change co-efficient between bubble and cloud

K_{ce} : Inter change co-efficient between cloud and emulsion

K_{f12} : Effective rate constant, s^{-1}

K_{r12} : Effective rate constant for the conversion of initial to inter mediate product, s^{-1}

K_{fAR} : Final rate constant for the process, s^{-1}

C_{A0} : Inter mediate concentration, mol/lit

C_{R0} : Final concentration, mol/lit

C_{Ai} : Initial concentration, mol/lit

S_R : Selectivity

X_A : Percentage conversion

L_f : Static bed height, m

v_p : Volume of particle, m^3

D_p : Diameter of particle, m

S_p : Surface of particle. m^2

ER : Equivalence ratio

Eu : Euler's number

H_s : Static bed height, m

d_p : Diameter of the bed materials, mm

D_c : Diameter of the fluidized bed column, cm

Subscripts

TGA : Thermo gravimetric analysis.

Exp : Values obtained through experimentally.

Cal : Values obtained through dimensionless analysis.

Prog : Values obtained through MAT LAB programming.

Dev : Deviation.

Greek Letters

τ : Reaction time, s

ε_e : Voidage of emulsion.

ε_f : Average bed voidage.

ε_{mf} : Voidage at the minimum fluidization condition.

δ : Fraction of bed in the bubble.

γ_b : Volume of solids dispersed in bubble / Volume of bubble.

γ_c : Volume of solids dispersed in cloud / Volume of bubble.

γ_e : Volume of solids dispersed in emulsion / Volume of bubble.

Φ_s : Sphericity of the particle.

ε : Void fraction.

ρ_s : Density of the solid materials, kg/m^3

ρ_f : Density of air, kg/m^3

ξ^2 : Chi-square.

η_c : Carbon conversion efficiency, %

References

[1] Fluidized bed reactor- http://en.wikipedia.org/wiki/Fluidized_bed_reactor, (2011).

[2] Aberuagba, F.,J.O. Odigure, K.R. Adeboye and M.A. Olutoye, "*Fluidization characteristics of a prototype fluidized bed reactor*", Federal University of Technology, Minna, Nigeria.

[3] Braun, R. L. and Burnham, A. K., "*Kinetics of Colorado fluidized-bed reactor oil, Lawrence Livermore National Laboratory*", Livermore, CA 94550, USA, 1985.

[4] Al-Zahrani, S. M., The effects of kinetics, "*Hydrodynamics and feed conditions onMethane coupling using fluidized bed reactor*", Catalysis today 64 (2001): pp. 217-225.

[5] Aldaco, R., Garea, A. and Irabien, A., "*Particle growth kinetics of calcium fluoride in a fluidized bed reactor*", Chemical Engineering Science 62, (2007): pp.2958-2966.

[6] Odedairo, T. and Al-Khattaf, S., "*Kinetic analysis of benzene ethylation over ZSM-5 based catalyst in a fluidized-bed reactor*", Chemical Engineering Journal 157(2010): pp.204-215.

[7] Wurzel, T., Malcus, S. and Mleczko, L., "*Reaction engineering investigations of CO_2 reforming in a fluidized-bed reactor*", Chemical Engineering Science 55(2000): pp.3955-3966.

[8] Fuertes, A. B., Marban, G. and Pis, J. J., "*Combustion kinetics of coke particles in a fluidized bed reactor*", Fuel Processing Technology 38 (1994): pp. 193-210.

[9] Ahchieva, D., Peglow, M., Heinrich, S., Morl, L., Wolff, T. and Klose, F., "*Oxidative dehydrogenation of ethane in a fluidized bed membrane reactor*", Applied Catalysis A: General 296 (2005): pp. 176-185.

[10] H. Zimmermann, R. Walzl, 6th rev. ed., ''*Ethylene in Ullmann's Encyclopedia of Industrial Chemistry*", vol. 12, Wiley VCH, (2003), pp.531–583.

[11] K. Weissermehl, H.-J.Arpe, "*Industrial Organic Chemistry*", 3rd rev.ed., Wiley VCH, Weinheim, (1999).

[12] Cave, S. R. and Holdich, R.G., "*The hydration kinetics of gypsum in a fluidized bed reactor*", Institution of Chemical Engineers Trans IChemE, Vol 78, (2000), Part A.

[13] Kelly, K. K., Southard, J. C. and Anderson, C. F., "*Fluidization Engineering*", US Bur Mines Tech Paper,(1941): pp.625.

[14] Hensen, F. E. and Clausen, H., "*Dehydration of gypsum*", ZemKalkGips, 26 (5)(1973): pp. 223-226.

[15] Kondrashenkov, A. A. and Bobov, E. A., "*Kinetics of the dehydration of gypsum in water vapour at 1208 ^{o}C to 2008 ^{o}C*", IzvAkadSSSR Neorg Mater, 16 (4)(1980): pp. 707-709.

[16] Khalil, A. A., "*Kinetics of gypsum dehydration*", ThermochimicaActa, 55 (1982): pp. 201-208.

[17] Holdridge D. A. and Walker, E. G., "*The Dehydration of Gypsum and Rehydration of Plaster*", Trans Brit Ceram Soc, 66 (10)(1967): pp. 485-509.

[18] Lavrov, M. N., "*Gypsum dehydration kinetics*", Uch Zap Gor'kGosPedagogInst, 73 (1968): pp. 101-115.

[19] Li, G. and Cao, Y., "*Dehydration of gypsum and its kinetics*", YankuangCeshi, 6 (4)(1987): pp.279-282.

[20] Bobrov, B. S., Zhigun, I. G., et al., "*Kinetics of the dehydration of $CaSO_4.2H_2O$*", IzvAkadNauk SSSR Neorg Mater, 14 (7)(1978): pp. 1333-1337.

[21] McAdie, H. G., "*The effect of water vapor upon the dehydration of $CaSO_4.2H_2O$*", Can J Chem., 42 (1964): pp. 792-801.

[22] Taylor, J. B and, Baines, J. E., "*Kinetics of the calcinations of calcium sulphatedehydrate*", J App.Chem., 20 (4)(1970): pp. 121-122.

[23] Brunello, S., Flour, I., Maissa, P., and Bruyet, B, "*Kinetic study of char combustion in a fluidized bed*", Elsevier Science Ltd.95 (1970): pp. 536-544.

[24] Rajgopal, S., Karthikeyan, T., Prakash Kumar, B.G. and Miranda, L. R., "*Utilization of fluidized bed reactor for the production of adsorbents in removal of malachite green*", Chemical Engineering Journal 116 (2006): pp. 211-217.

[25] A.K. Jain, V.K. Gupta, A. Bhatnagar, Suhas, "*Utilization of industrial waste product as adsorbents for the removal of dyes*", J. Hazard.Mater. B 101 (2003): pp. 31–42.

[26] Li, Y. H, Lu, G. Q. and Rudolph, V., "*The kinetics of NO and N2O reduction over coal chars in fluidized-bed combustion*", Chemical Engineering science 53 (1998): pp. 1-26.

[27] Khani, M. H., Pahlavanzadeh, H., Ghannadi, M., "*Kinetics study of the fluorination of uranium tetra fluoride in a fluidized bed reactor*", Annals of nuclear energy 35 (2008): pp. 704-707.

[28] Lee, J. M., Kim, Y. J., Lee, W. J. and Kim, S. D., "*Coal-gasification kinetics derived from pyrolysis in a fluidized bed reactor*", Elsevier Science Ltd. 23 (1998): pp. 475-488.

[29] Luo, Z., Wang, S. and Cen, K., "*A model of wood flash pyrolysis in fluidized bed reactor*", Renewable Energy 30 (2005): pp. 377-392.

[30] Chiovetta, M. G., Romero, R. L. and Cassano, A. E., "*Influence of Pretreatment of Titanium Substrate on Long-Term Stability of TiO_2 Film*", Chemical Engineering Science 56 (2001): pp. 1631-1638.

[31] Mohanty, Y. K., Mohanty, B. P., Roy, G. K. and Biswal, K. C., "*Effect of secondary fluidizing medium on hydrodynamics of gas-solid fluidized bed- statistical and ANN approaches*", Chemical Engineering Journal 148 (2009): pp. 41-49.

[32] Papadikis, K., Gu, S. and Bridgwater, A. V., "*Computational modeling of the impact of particle size to the heat transfer coefficient between biomass particles and a fluidized bed*", Fuel processing technology 91 (2010): pp. 68-79.

[33] Lu, W. Z., Teng, L. H. and Xiao, W. D., "*Simulation and experimental study of dimethyl ether synthesis from syngasin a fluidized-bed reactor*", Chemical Engineering Science 59 (2004): pp. 5455 – 5464.

[34] Lv, P. M., Z. H. Xiong, J. Chang, C. Z. Wu, Y. Chen, J.X. Zhu, "*An experimental study on Biomass air-steam gasification in a fluidized bed*", Bioresource Technology 95 (2004): pp. 95-101.

[35] Ikeda, Y., Kagaku, K., "*Fluidization Engineering*", Fukui City, Japan, Elsevier, 34 (1970): pp. 1013.

[36] Davidson, J. F. and D. Harrison, "*Fluidized particles*", Cambridge University Press, New York, (1963).

[37] Werther, J., in fluidization IV, D. Kunni and R. Toei, eds., "*Engineering Foundation*", New York, (1983): pp. 93.

[38] Kunni, D. and Levenspiel, O., "*Fluidization Engineering*", Fukui City, Japan, Elsevier, (2005).

[39] T. Chiba and H. Kobayashi,"*A revised model for predicting the performance of a fluidised-bed catalytic reactor*",Chem. Engg. Sci., 25 (1970): pp. 1375.

[40] Gupta, O. P., "*Elements of fuels, furnaces and refractories*", Bokaro Steel City, Khanna Publishers, (2000).

[41] McCabe, W. L., Smith, J. C. and Harriott, P., "*Unit operations of chemical engineering*", New York, McGraw-Hill publication, (1993): pp. 928.

[42] Kumar, A., "*Effect of promoter and distributor parameters on the performance of gas-solid fluidized beds*", Ph.D. thesis, Department of applied mechanics and hydraulics, National Institute of Technology, Rourkela, May (2003).

Appendix

Annexure-1

MAT LAB CODING:

```
%programme for fluidised bed reactor
clc
display('enter the values of required parameters(m)=')
dp=input('enter the value of particle size=')
epsilonm=input('enter the value of epsilonm=')
epsilonmf=input('enter the value of epsilonmf=')
Umf=input('enter the value of Umfim m/s=')
Da=input('enter the value of Da=')
Dr=input('enter the value of Dr=')
Ds=input('enter the value of Ds=')
gammab=input('enter the value of gammab=')
Kr12=input('enter the value of Kr12=')
Fw=input ('enter the value of Fw=')
display('for pilot plant')
N=6;
U0=zeros(N,1)
Kf12=zeros(N,1)
floatepsilonfU0;
display('for pilot plant')
db=input('enter the value of db=')
dte=input('enter the value of dte=')
Ubr=0.711*((9.8*db).^0.5);
for i=1:1:N;
U0(i)=0.1*i;
display(U0(i));
Ub=1.55*((U0(i)-Umf)+14.1*(db+0.005))*(dte.^0.32)+Ubr;
delta=(U0(i)/Ub);
epsilonf=1-((1-delta)*(1-epsilonmf));
gammac=(1-epsilonmf)*(3/(Ubr*(epsilonmf/Umf)-1)+Fw);
gammae=(((1-epsilonmf)*(1-delta))/delta)-gammab-gammac;
Kbc=4.5*(Umf/db)+5.85*(Da^(0.5)*9.8^(0.25)/(db^(1.25)));
Kce=6.77*((Da*epsilonmf*Ubr/(db^3))^0.5);

Kf12(i)=(gammab*Kr12+(1/((1/Kbc)+(1/(gammac*Kr12+((1/Kce)+(1/(gammae*Kr12))))
))))*(delta/(1-epsilonf))
end
%gammac=volume of solids dispersed in cloud phase/volume of bubbles.
%gammab=volume of solids dispersed in bubble phase/volumes of bubbles.
%gammae=volume of solids dispersed in emulision phase/volume of bubbles.
display('for laboratory unit')
M=6;
U0=zeros(M,1)
K1f12=zeros(M,1)
floatepsilonfU0;
display('for laboratiry unit')
db=input('enter the value of db=')
dte=input('enter the value of dte=')
Ubr=0.711*((9.8*db).^0.5);
for j=1:1:M;
U0(j)=0.1*j;
display(U0(j));
```

```
Ub=1.55*((U0(j)-Umf)+14.1*(db+0.005))*(dte.^0.32)+Ubr;
delta=(U0(j)/Ub);
epsilonf=1-((1-delta)*(1-epsilonmf));
gammac=(1-epsilonmf)*(3/(Ubr*(epsilonmf/Umf)-1)+Fw);
gammae=(((1-epsilonmf)*(1-delta))/delta)-gammab-gammac;
Kbc=4.5*(Umf/db)+5.85*(Da^(0.5)*9.8^(0.25)/(db^(1.25)));
Kce=6.77*((Da*epsilonmf*Ubr/(db^3))^0.5);

K1f12(j)=(gammab*Kr12+(1/((1/Kbc)+(1/(gammac*Kr12+((1/Kce)+(1/(gammae*Kr12)))
)))))*(delta/(1-epsilonf))
end
display('for semi commercial use')
L=6;
U0=zeros(L,1)
K2f12=zeros(L,1)
floatepsilonfU0;
display('for semi commercial unit')
db=input('enter the value of db=')
dte=input('enter the value of dte=')
Ubr=0.711*((9.8*db).^0.5);
for k=1:1:L;
U0(k)=0.1*k;
display(U0(k));
Ub=1.55*((U0(k)-Umf)+14.1*(db+0.005))*(dte.^0.32)+Ubr;
delta=(U0(k)/Ub);
epsilonf=1-((1-delta)*(1-epsilonmf));
gammac=(1-epsilonmf)*(3/(Ubr*(epsilonmf/Umf)-1)+Fw);
gammae=(((1-epsilonmf)*(1-delta))/delta)-gammab-gammac;
Kbc=4.5*(Umf/db)+5.85*(Da^(0.5)*9.8^(0.25)/(db^(1.25)));
Kce=6.77*((Da*epsilonmf*Ubr/(db^3))^0.5);

K2f12(k)=(gammab*Kr12+(1/((1/Kbc)+(1/(gammac*Kr12+((1/Kce)+(1/(gammae*Kr12)))
)))))*(delta/(1-epsilonf))
end
plot(U0,Kf12,'r',U0,K1f12,'b',U0,K2f12,'g');
xlabel('velocity(m/s)');
ylabel('rate constant(1/s)');
title('rate constant vs velocity characteristics ');
%%%%%%%%%%%%%%%%%%%%%%%%%%%%%%%%%%%%%%%%%%%%%%%%%%%%%%%%%%%%%%%%%%%%%%%%%%%%
display('for selectivity vs conversion')
display('for pilot plant')
Kr1=input('enter the value of Kr1=')
Kr3=input('enter the value of Kr3=')
delta1=input('enter the value of delta1=')
Y=8;
Xa=zeros(Y,1)
tou=zeros(Y,1)
% B=Cr/Cai;
B=zeros(Y,1)
Sr=zeros(Y,1)
kf12=input('enter the value of kf12=')
KfAR=(Kr1/Kr12)*kf12
Kf3=(gammab*Kr3+1/((1/Kbc)+(1/(gammac*Kr3+(1/((1/Kce)+(1/(gammae*Kr3)))))))))*
(delta1/(1-epsilonf))
for h=1:1:Y;
Xa(h)=0.01*h+0.8;
display(Xa(h))
```

```
tou(h)=-2.303*((log(1-Xa(h)))/(kf12))
B(h)=(KfAR/(Kf3-kf12))*(exp(-kf12*tou(h))-exp(Kf3*tou(h)))
%B(h)=Cr/Cai
Sr(h)=B(h)/Xa(h)
end
Z=8;
Xa=zeros(Z,1)
tou=zeros(Z,1)
% B=Cr/Cai;
B=zeros(Z,1)
S1r=zeros(Z,1)
k1f12=input('enter the value of k1f12=')
KfAR=(Kr1/Kr12)*k1f12
Kf3=(gammab*Kr3+1/((1/Kbc)+(1/(gammac*Kr3+(1/((1/Kce)+(1/(gammae*Kr3))))))))*
(delta1/(1-epsilonf))
for f=1:1:Z;
Xa(f)=0.01*f+0.8;
display(Xa(f))
tou(f)=-2.303*((log(1-Xa(f)))/(k1f12))
B(f)=(KfAR/(Kf3-k1f12))*(exp(-k1f12*tou(f))-exp(Kf3*tou(f)))
%B(h)=Cr/Cai
S1r(f)=B(f)/Xa(f)
end
W=8;
Xa=zeros(W,1)
tou=zeros(W,1)
% B=Cr/Cai;
B=zeros(W,1)
S2r=zeros(W,1)
k2f12=input('enter the value of k2f12=')
KfAR=(Kr1/Kr12)*k2f12
Kf3=(gammab*Kr3+1/((1/Kbc)+(1/(gammac*Kr3+(1/((1/Kce)+(1/(gammae*Kr3))))))))*
(delta1/(1-epsilonf))
for o=1:1:W;
Xa(o)=0.01*o+0.8;
display(Xa(o))
tou(o)=-2.303*((log(1-Xa(o)))/(k2f12))
%B(h)=Cr/Cai
S2r(o)=B(o)/Xa(o)
end
plot(Xa,Sr,'r',Xa,S1r,'b',Xa,S2r,'g')
xlabel('conversion(XA)');
ylabel('selectivity(Sr)');
title('selectivity vs conversion characteristics')
%%%%%%%%%%%%%%%%%%%%%%%%%%%%%%%%%%%%%%%%%%%%%%%%%%%%%%%%%%%%%%%%%%%%%%%%%%%%%%%
display('programme for touvs XA')
K=input('enter the value of rate constant(K)=')
k=9;
tou=zeros(k,1)
XA=zeros(k,1)
for s=1:1:9;
tou(s)=1*s
    XA(s)=1-exp(-K*tou(s))
end
K1=input('enter the value of rate constant(K1)=')
k1=9;
tou1=zeros(k1,1)
```

```
XA1=zeros(k1,1)
for s1=1:1:9;
tou1(s1)=1*s1
XA1(s1)=1-exp(-K1*tou1(s1))
end
K2=input('enter the value of rate constant(K2)=')
k2=9;
tou2=zeros(k2,1)
XA2=zeros(k2,1)
for s2=1:1:9;
tou2(s2)=1*s2
XA2(s2)=1-exp(-K2*tou2(s2))
end

plot(tou,XA,'r',tou1,XA1,'g',tou2,XA2,'b');
xlabel('time(s)');
ylabel('conversion(XA)');
title('conversion vs time characteristics')
%%%%%%%%%%%%%%%%%%%%%%%%%%%%%%%%%%%%%%%%%%%%%%%%%%%%%%%%%%%%%%%%%%%%%%%%%%%%%%%
display('programme for bed height vs XA')
U0=input('enter the value of U0=')
K=input('enter the value of rate constant(K)=')
X=10;
tou=zeros(X,1)
Lf=zeros(X,1)
xA=zeros(X,1)
for m=1:1:10
tou(m)=1*m
Lf(m)=tou(m)*U0/(1-epsilonf)
xA(m)=1-exp(-K*tou(m))
end
K1=input('enter the value of rate constant(K1)=')
Y=10;
tou1=zeros(Y,1)
Lf1=zeros(Y,1)
xA1=zeros(Y,1)
for n=1:1:10
tou(n)=1*n
Lf1(n)=tou(n)*U0/(1-epsilonf)
xA1(n)=1-exp(-K1*tou(n))
end
K2=input('enter the value of rate constant(K2)=')
Z=10;
tou2=zeros(Z,1)
Lf2=zeros(Z,1)
xA2=zeros(Z,1)
for p=1:1:10
tou(p)=1*p
Lf2(p)=tou(p)*U0/(1-epsilonf)
xA2(p)=1-exp(-K2*tou(p))
end
plot(Lf,xA,'g',Lf1,xA1,'r',Lf2,xA2,'b')
xlabel('bed height(Lf)');
ylabel('conversion(XA)')
title('conversion vs bed height characteristics')
```